

# Performance Investigation of Vector Controlled Induction Motor Drive Using Sensorless Speed Estimation Techniques

A DISSERTATION

*Submitted in partial fulfillment of the requirements for the award of the degree*

*of*

MASTER OF TECHNOLOGY

*in*

ELECTRICAL ENGINEERING

(With specialization in Electric Drives And Power Electronics)

*By*

MINTU MUNSHI



DEPARTMENT OF ELECTRICAL ENGINEERING  
INDIAN INSTITUTE OF TECHNOLOGY ROORKEE  
ROORKEE - 247 667 (INDIA)

MAY, 2016

## CANDIDATE'S DECLARATION

I hereby declare that this thesis report entitled **Performance Investigation of Vector Controlled Induction Motor Drive Using Sensorless Speed Estimation Techniques**, submitted to the Department of Electrical Engineering, Indian Institute of Technology, Roorkee, India, in partial fulfillment of the requirements for the award of the Degree of Master of Technology in Electrical Engineering with specialization in Electric Drives and Power Electronics is an authentic record of the work carried out by me during the period June 2015 through May 2016, under the supervision of **Dr. Sumit Ghatak Choudhuri, Department of Electrical Engineering, Indian Institute of Technology, Roorkee**. The matter presented in this thesis report has not been submitted by me for the award of any other degree of this institute or any other institutes.

Date:

Place: Roorkee

**Mintu Munshi**

## CERTIFICATE

This is to certify that the above statement made by the candidate is true to the best of my knowledge and belief.

**Dr. Sumit Ghatak Choudhuri**

Assistant Professor

Department of Electrical Engineering

Indian Institute of Technology Roorkee

# ABSTRACT

It has become a common practice for the industry to use vector control technique in induction motor control. In this method stator current space vector is decoupled into two components in synchronously rotating reference frame where one component provides control over flux and the other controls the torque in an independent way like a DC machine. That is why, With the help of this control technique the induction motor can fill the role of a separately excited dc motor. Existence of commutator, brushes, brush holders in dc motor makes dc motor drive less reliable as it calls for time to time maintenance. Henceforth the main effort is to replace DC motor by an induction motor and merge the advantages of both the motor together into the variable speed brushless motor drive and eliminate the associated problems. The squirrel cage induction motor being simple, rugged, and cheap, and requiring less maintenance, has been widely used for fixed speed applications. So implementation of vector control technique is an attractive solution for creating two independent channels so as to control flux and torque independently which in turn makes the induction motor from a non-linear to linear plant. However, the essential requirement for the proper operation of the vector controller is precise knowledge of rotor flux position which demands a speed sensor (e.g. shaft mounted tachogenerators, resolvers, search coils or digital shaft position encoder). These cause the system to be less reliable and lose benefits of an induction motor drive as well. Sensorless vector control came as a solution of the aforesaid problem in which the speed is estimated using some of the estimation methods rather than using speed sensors. In this dissertation work a scheme of open loop speed estimator using stator voltage and current and MODEL REFERENCE ADAPTIVE SYSTEM (MRAS) based speed estimators are proposed and simulated in Simulink/Matlab environment and performance of these schemes are evaluated on various operating conditions.

## *Acknowledgements*

I would like to express my deep sense of gratitude and sincere thanks to my guide **Dr. Sumit Ghatak Choudhuri**, Department of Electrical Engineering, Indian Institute of Technology Roorkee, for his valuable guidance and support. I am highly indebted to him for his encouragement and constructive criticism throughout the course of this project work. In spite of his hectic schedule, he was always there for clarifying my doubts and reviewed my dissertation progress in a constructive manner. Without his help, this thesis would not have been possible.

**Mintu Munshi**

# Contents

<b>Candidate's Declaration</b>	<b>i</b>
<b>Abstract</b>	<b>ii</b>
<b>Acknowledgements</b>	<b>iii</b>
<b>List of Figures</b>	<b>vi</b>
<b>List of Symbols</b>	<b>viii</b>
<b>1 INTRODUCTION</b>	<b>1</b>
1.1 VECTOR CONTROL OF INDUCTION MOTOR . . . . .	2
1.1.1 Classification of Vector Control Technique . . . . .	3
1.2 SPEED SENSORLESS AC DRIVE . . . . .	4
1.3 MAIN OBJECTIVE OF SENSORLESS DRIVE . . . . .	4
1.4 SENSORLESS SPEED ESTIMATORS . . . . .	5
1.4.1 Open Loop Speed Estimator . . . . .	5
1.4.2 Model Reference Adaptive System(MRAS) . . . . .	5
1.5 ORGANISATION OF THE REPORT . . . . .	6
<b>2 LITERATURE REVIEW</b>	<b>7</b>
2.1 INTRODUCTION . . . . .	7
2.2 SIGNIFICANT DEVELOPMENTS . . . . .	7
2.3 LITERATURE REVIEW . . . . .	8
<b>3 MATHEMATICAL MODELING OF VECTOR CONTROLLED IN- DUCTION MOTOR DRIVE</b>	<b>10</b>
3.1 SPEED CONTROLLER . . . . .	10
3.2 LIMITER . . . . .	10
3.3 FIELD WEAKENING CONTROL . . . . .	11
3.4 VECTOR CONTROL STRUCTURE . . . . .	11
3.4.1 Modeling of Vector Controller . . . . .	12
3.5 INVERSE CLARKE'S AND PARK'S TRANSFORMATION . . . . .	14
3.6 CURRENT CONTROLLER . . . . .	15

3.6.1	Modeling of Pulse Width Modulated(PWM) Current Controller (CC) . . . . .	15
3.7	CURRENT CONTROLLED VOLTAGE SOURCE INVERTER . . . . .	16
3.7.1	Modeling of Voltage Source Inverter(VSI) . . . . .	16
3.8	INDUCTION MOTOR . . . . .	17
3.8.1	Modeling of Induction Motor . . . . .	17
<b>4</b>	<b>SPEED ESTIMATION SCHEMES</b>	<b>18</b>
4.1	OPEN LOOP SPEED ESTIMATOR . . . . .	18
4.1.1	CALCULATION OF SPEED . . . . .	19
4.1.1.1	Calculation of Rotor Flux( $\psi_{\alpha r}$ and $\psi_{\beta r}$ ) . . . . .	19
4.1.1.2	Calculation of Angular Rotor-Slip Speed( $\omega_{sl}$ ) . . . . .	19
4.1.2	Simulation Block of Open Loop Speed Estimator . . . . .	21
4.2	MRAS BASED SPEED ESTIMATOR . . . . .	22
4.2.1	Rotor flux based MRAS . . . . .	23
4.2.1.1	Reference Model . . . . .	23
4.2.1.2	Adaptive Model . . . . .	23
4.2.1.3	Simulation Block of RF-Based Speed Estimator . . . . .	24
4.2.2	Back EMF based MRAS . . . . .	25
4.2.2.1	Reference Model . . . . .	25
4.2.2.2	Adaptive Model . . . . .	25
4.2.2.3	Simulink Block of Back-Emf Based Speed Estimator . . . . .	26
4.2.3	Airgap reactive power based MRAS . . . . .	27
4.2.3.1	Reference Model . . . . .	27
4.2.3.2	Adaptive Model . . . . .	27
4.2.3.3	Simulink Block of Airgap Reactive Power Based MRAS . . . . .	28
<b>5</b>	<b>RESULTS &amp; DISCUSSIONS</b>	<b>30</b>
5.1	STARTING DYNAMICS . . . . .	30
5.1.1	Results Starting Dynamics . . . . .	31
5.2	LOAD PERTURBATION . . . . .	37
5.2.1	Results of load Perturbation . . . . .	37
5.3	FOUR QUADRANT OPERATION . . . . .	39
5.3.1	Results of Four Quadrant Operation of IM . . . . .	40
<b>6</b>	<b>CONCLUSIONS &amp; FUTURE SCOPE OF WORK</b>	<b>42</b>
6.1	CONCLUSIONS . . . . .	42
6.2	FUTURE SCOPE OF WORK . . . . .	43
	<b>Bibliography</b>	<b>44</b>
	<b>Appendix I</b>	<b>50</b>
	<b>Appendix II</b>	<b>51</b>

# List of Figures

1.1	Simplified Schematic for Vector Controlled Induction Motor . . . . .	3
1.2	MRAS Based Speed Estimation Scheme . . . . .	6
3.1	Vector Controller Subsystem(A) . . . . .	13
3.2	Vector Controller Subsystem(B) . . . . .	13
3.3	Vector Controller Subsystem(C) . . . . .	13
3.4	Vector Controller . . . . .	14
3.5	Two Phase Rotating Frame to Three Phase Stationary Frame Converter .	14
3.6	PWM Generator . . . . .	16
4.1	Vector Diagram of Relevent Phasors . . . . .	18
4.2	Block Diagram of Open Loop Speed Estimator . . . . .	21
4.3	Simulink Block Diagram for Flux Calculator Used in Speed Estimator Block	22
4.4	Simulink Block Diagram For Speed Estimation . . . . .	22
4.5	MRAS Based Speed Estimation Scheme . . . . .	23
4.6	Block Diagram of RF Based Speed Estimator . . . . .	24
4.7	Simulink Reference model of RF based MRAS . . . . .	25
4.8	Simulink Adaptive model of RF based MRAS . . . . .	25
4.9	Block Diagram of back emf Based Speed Estimator . . . . .	26
4.10	Simulink reference model of back EMF based MRAS . . . . .	27
4.11	Simulink Adaptive model of back EMF based MRAS . . . . .	27
4.12	Block Diagram airgap reactive power based Speed Estimator . . . . .	28
4.13	Simulink Reference model of Airgap power based MRAS . . . . .	29
4.14	Simulink Adaptive model of Airgap power based MRAS . . . . .	29
5.1	Starting dynamics of open loop speed estimator with $\omega_r = 250rad/sec(30hp)$	31
5.2	Starting dynamics of open loop speed estimator with $\omega_r = 20rad/sec(30hp)$	31
5.3	Starting dynamics of RF-based speed estimator with $\omega_r = 250rad/sec(30hp)$	31
5.4	Starting dynamics of RF-based speed estimator with $\omega_r = 20rad/sec(2hp)$	31
5.5	Starting dynamics of Back Emf based speed estimator with $\omega_r = 250rad/sec(2hp)$	32
5.6	Starting dynamics of Back Emf based speed estimator with $\omega_r = 250rad/sec(30hp)$	32
5.7	Starting dynamics of Back Emf based speed estimator with $\omega_r = 40rad/sec(2hp)$	32
5.8	Starting dynamics of Back Emf based speed estimator with $\omega_r = 20rad/sec(30hp)$	32
5.9	Starting dynamics of reactive power based speed estimator with $\omega_r =$ $250rad/sec(30hp)$ . . . . .	33
5.10	Starting dynamics of reactive power based speed estimator with $\omega_r =$ $40rad/sec(30hp)$ . . . . .	33

5.11 Starting dynamics of reactive power based speed estimator with $\omega_r = 20rad/sec(2hp)$ . . . . .	33
5.12 Starting dynamics of RF-based speed estimator with $1.2R_s \omega_r = 250rad/sec(30hp)$	33
5.13 Starting dynamics of open loop speed estimator with $1.2R_s$ and $\omega_r = 40rad/sec(30hp)$ . . . . .	34
5.14 Starting dynamics of open loop speed estimator with $1.2R_s$ and $\omega_r = 250rad/sec(30hp)$ . . . . .	34
5.15 Starting dynamics of RF-based speed estimator with $1.2R_s$ and $\omega_r = 100rad/sec(30hp)$ . . . . .	34
5.16 Starting dynamics of RF-based speed estimator with $1.2R_s \omega_r = 20rad/sec(2hp)$	34
5.17 Starting dynamics of Back Emf based speed estimator with $1.2R_s$ and $\omega_r = 250rad/sec(30hp)$ . . . . .	35
5.18 Starting dynamics of Back Emf speed estimator with $1.2R_s$ and $\omega_r = 40rad/sec(30hp)$ . . . . .	35
5.19 Starting dynamics of Bemf-based speed estimator with $1.2R_s$ and $\omega_r = 250rad/sec(2hp)$ . . . . .	35
5.20 Starting dynamics of Bemf-based speed estimator with $1.2R_s \omega_r = 40rad/sec(2hp)$	35
5.21 Starting dynamics of reactive power based speed estimator with $1.2R_s$ and $\omega_r = 250rad/sec(30hp)$ . . . . .	36
5.22 Starting dynamics of reactive power based speed estimator with $1.5R_s \omega_r = 40rad/sec(30hp)$ . . . . .	36
5.23 Starting dynamics of reactive power based speed estimator with $1.5R_s$ and $\omega_r = 250rad/sec(30hp)$ . . . . .	36
5.24 Starting dynamics of reactive power based speed estimator with $1.5R_s \omega_r = 20rad/sec(2hp)$ . . . . .	36
5.25 Load perturbation of RF-based speed estimator with $\omega_r = 250rad/sec(2hp)$	37
5.26 Load perturbation of RF-based speed estimator with $\omega_r = 250rad/sec(30hp)$	37
5.27 Load perturbation of RF-based speed estimator with $\omega_r = 20rad/sec(2hp)$	38
5.28 Load perturbation of RF-based speed estimator with $\omega_r = 20rad/sec(30hp)$	38
5.29 Load perturbation of Back Emf-based speed estimator with $\omega_r = 20rad/sec(2hp)$	38
5.30 Load perturbation of Back Emf based speed estimator with $\omega_r = 20rad/sec(30hp)$	38
5.31 Load perturbation of reactive power based speed estimator with $\omega_r = 20rad/sec(2hp)$ . . . . .	39
5.32 Load perturbation of Back Emf based speed estimator with $\omega_r = 250rad/sec(2hp)$	39
5.33 Performance of open loop speed estimator with $\omega_r = \pm 100rad/sec(30hp)$ .	40
5.34 Performance of RF-based speed estimator with $\omega_r = \pm 250rad/sec(30hp)$ .	40
5.35 Performance of RF-based speed estimator with $\omega_r = \pm 20rad/sec(30hp)$ .	40
5.36 Performance of RF-based speed estimator with $\omega_r = \pm 20rad/sec(2hp)$ . .	40
5.37 Performance of Back-Emf based estimator with $\omega_r = \pm 20rad/sec(30hp)$ .	41
5.38 Performance of reactive power-based speed estimator with $\omega_r = \pm 20rad/sec(2hp)$	41



# List of Symbols

$i_{as}, i_{bs}, i_{cs}$	Stator currents in stationary reference frame.
$i_{as}^*, i_{bs}^*, i_{cs}^*$	Stator reference currents in stationary reference frame.
$i_{\beta s}$ OR $i_{qss}$	Q-axis component of stator current in stationary reference frame.
$i_{\alpha s}$ OR $i_{dss}$	D-axis component of stator current in stator reference frame.
$v_{\beta s}$ OR $v_{qss}$	Q-axis component of stator voltage in stationary reference frame.
$v_{\alpha s}$ OR $v_{dss}$	D-axis component of stator voltage in stationary reference frame.
$\omega_r$	Rotor speed (rad/sec).
$\omega_e$	Synchronous speed (rad/sec).
$\omega_{sl}$	Slip speed (rad/sec).
$i_{qs}$	Q-axis component of stator current in synchronous reference frame.
$i_{ds}$	D-axis component of stator current in synchronous reference frame.
$\psi_{\alpha s}, \psi_{\alpha r}$	D-axis component of stator and rotor flux in stationary reference frame.
$\psi_{\beta s}, \psi_{\beta r}$	Q-axis component of stator and rotor flux in stationary reference frame.
$\rho_r$	Field angle.
$L_{ls}, L_{lr}$	Leakage inductance of stator and rotor.
$L_m$	Mutual inductance.
$L_s, L_r$	Stator and rotor self-inductance.
$R_s, R_r$	Stator and rotor resistance.
$\tau_r$	Rotor time constant.
$\sigma$	Total leakage factor.
$J$	Moment of inertia.

# Chapter 1

## INTRODUCTION

---

Faraday discovered electromagnetic induction in 1831. After this discovery, it took about fifty years when Nicholas Tesla invented induction machine in 1888. This newly invented brushless AC machine was the reason for the revolution in electrical engineering, gave a scope for its wide spread use in polyphase generation and distribution system. The grid frequency (50  $Hz$  in Asia and Europe, 60  $Hz$  in USA) was determined in 19<sup>th</sup> century as Tesla found this frequency suitable for his induction machine design.

Nowadays major portion of the energy is generated, being used by cage induction motor and that is why induction motor is called work horse of the industry. The squirrel cage induction motor is preferred due its simple construction, ruggedness, reliability, higher efficiency, low cost less financial support to keep it in service. It has been the most sought-after motor for fixed speed applications. Unlike induction machine DC machines have been used for variable speed drive because of its inherent simplicity in its control of speed. Number of attempts have been made to substitute 3 –  $\phi$  squirrel cage induction motors in variable speed drive applications, wherein the genuine choice has been for dc motors. But DC motor has some serious issues with commutators and brushes as these call for frequent maintenance. Therefore, the main basis of the efforts is to replace dc machine by an induction machine so as to integrate the advantages of both the motors together into a variable speed brushless motor drive and remove the associated problems.

Even though induction motor is a better choice over DC motor with respect to cost, reliability, weight, size, but its non-linear nature demands complex control strategy for its

speed control. Rapid development of power electronics devices such as IGBT, MOSFET made it possible to implement complex control strategy for the control purpose of induction machine.

In variable speed drive the genuine choice of separately excited DC motor is because of its ease of speed control as the field and armature currents are electrically decoupled from each other. Now in present scenario, when all the latest tools of power electronics technology are available, there is need for simplicity and economic feasibility of the control technique. Therefore, it is to develop a proper and adequate control technique for controlling the relevant induction motor variables namely, frequency and slip which would enable the motor to operate as variable speed drive.

Scalar control is used for speed control of induction motor where magnitude of voltage is basically used as control variable below base speed keeping air-gap flux constant to achieve maximum torque for a fixed level of flux. Constant flux is achieved through maintaining the ratio of voltage to frequency constant with a boost at lower frequencies for resistive effects. Scalar control is possible in open loop or close loop manner. In case of close loop accuracy is more as compared to open loop control. At steady state, torque becomes linear with slip below the peak torque limit. And this draws the simplicity in control. Even though scalar control is very simple to implement but it suffers from poor dynamic response. And that is why in many control application DC motor wins over induction motor. Vector control technique came as a solution of poor dynamic response for induction motor control where control of flux and torque becomes completely independent to each other. As a result induction motor operating in vector control mode start behaving just like a separately excited DC motor for variable speed drive. Thus vector control makes it possible to merge all the advantages of induction machine and DC machine in a variable speed drive.

## 1.1 VECTOR CONTROL OF INDUCTION MOTOR

Unlike scalar control, vector control is a control technique which decouples the stator current space vector in synchronously rotating reference frame (SRRF) where one component is used for controlling flux and other for controlling torque. This decoupled form of flux and torque control makes induction motor (IM) a nonlinear to linear plant helping it to run as separately excited DC motor. In SRRF, decoupled components of stator

current space vector matches with the two current components as commanded by the vector controller. An induction motor operating under vector control mode is shown in figure 1.1. To perform vector control, speed is sensed and fed back to the controller. The controller gives two decoupled reference components of stator current in SRRF namely  $i_{qs}^*$  and  $i_{ds}^*$  for the torque and flux control respectively. Then inverse park and clarke transform generates three reference values of currents ( $i_{as}^*, i_{bs}^*, i_{cs}^*$ ) in stationary reference frame (SRF). As IM is a three phase balanced load, sensing of two phase current is sufficient for its vector control. The current controller ensures three phase currents to follow reference currents closely in SRF and drives the voltage source inverter (VSI) to come in operation so as to feed the 3- $\phi$  induction motor. This way motor currents are forced to follow the reference currents which gives higher dynamic performance of induction motor (IM) operating in vector control mode. Such drives are becoming popular in the fields of many drive application such as air conditioning refrigerators, fan, blowers, pumps, waste water treatment plants, elevators, lifts, traction, electrical vehicles etc.

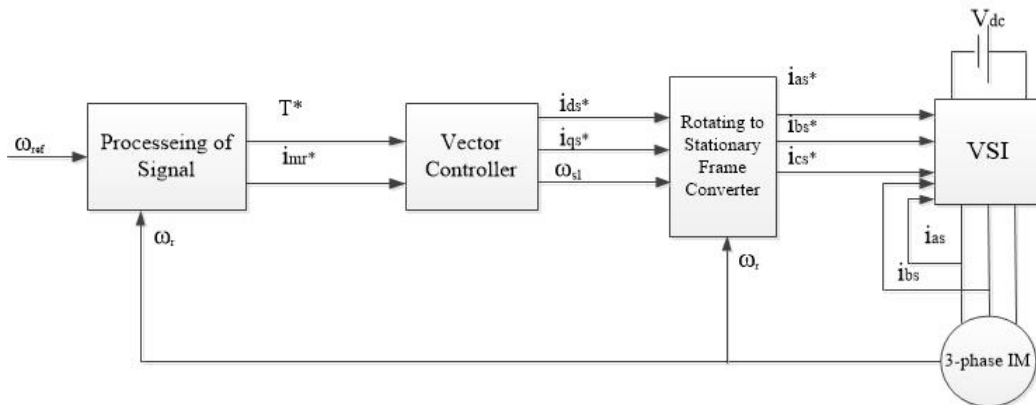


FIGURE 1.1: Simplified Schematic for Vector Controlled Induction Motor

### 1.1.1 Classification of Vector Control Technique

For realization of vector control technique, SRRF can be set along the rotor flux, stator flux or magnetizing flux space vector respectively. Depending upon the alignment of SRRF, vector control is known as rotor, stator or magnetizing flux oriented control. It has been observed that when SRRF is aligned with rotor flux space vector, control becomes simpler and shows better dynamic performance as compared to other alignments of SRRF. Based on how field angle is achieved, vector control technique can be classified into two categories a) Direct vector control b) Indirect vector control. In Direct vector control position of flux vector is obtained by direct measurement of flux or estimation. Flux can be measured by using sensors (e.g. hall effect sensors, search coils, tapped

stator windings of the machine etc). On the other hand estimation of flux is possible by using a flux model which consists of motor parameters and electrical inputs. The major pitfall of this method is the need of several sensors which makes it infamous for using in motors. For flux measurement, sensors are needed to fix up in stator structure which calls for extra manufacturing cost and reduces robustness of the machine. It also suffers from the problem of drift because of temperature and inability of flux sensing at low speed also persists. In indirect vector control position of rotor flux vector is determined from speed signal feedback rather than sensing it directly using sensors and that's why this method is known as indirect vector control. This way, indirect vector control solves the problem of flux sensors as the controller is freed from rotor flux sensing now. Below base speed rotor flux is maintained constant by controlling the in phase component in SRRF while quadrature component of stator current space vector is used for the production of torque. Henceforth, such control technique replaces a separately excited DC motor with the use of  $3 - \phi$  squirrel cage induction motor in variable speed ac drive.

## 1.2 SPEED SENSORLESS AC DRIVE

In past few decades collective endeavour of researchers made it possible to introduce sensorless torque controlled (vector or direct torque control) drive. The terminology not only refers to the speed sensor it includes other sensors such as current sensor, voltage sensor as well which is necessary for close loop operation of the drive. Because of reduced hardware complexity, and cost, increased robustness, sensorless drive has become a normal practice in almost all large manufactures (Control Technique plc, Simens, Hitachi, Yaskawa Eurotherm etc.). Elimination of speed sensor is also desirable from the point of view of noise immunity. In real time computation the objective is towards in computation of speed from minimum sensed signals.

## 1.3 MAIN OBJECTIVE OF SENSORLESS DRIVE

The main objective of Sensorless drive control are:

- Reduction of hardware complexity and cost.
- Increased mechanical robustness and overall ruggedness.
- Operation in hostile environments.

- Higher reliability.
- Decreased maintenance requirements.
- Increased noise immunity.

## 1.4 SENSORLESS SPEED ESTIMATORS

- Open Loop Speed Estimator
- Model Reference Adaptive System(MRAS) based Speed Estimator
  1. Rotor flux based MRAS.
  2. Back EMF based MRAS.
  3. Air-gap reactive power based MRAS.
- Observer based speed estimator(Kalman,Luenberger).
- Estimator using artificial intelligence (Newral network, Fuzzy-logic-based systems, Fuzzy-newral networks etc.)
- Estimator using saliency(geometrical, saturation) effects.

### 1.4.1 Open Loop Speed Estimator

In this technique rotor speed is obtained directly from voltage model of induction machine. The scheme uses monitored stator voltage and currents for estimating speed. But the speed estimation with this voltage model greatly depends on machine parameter used, which reduces the accuracy of speed estimation. Accuracy of stator resistance ( $R_s$ ), determines the accuracy of estimated speed as stator resistance has great effect of stator as well as rotor flux estimation.

### 1.4.2 Model Reference Adaptive System(MRAS)

Accuracy of open loop speed estimator significantly depends on machine parameters used. Accuracy can be increased if speed is estimated in close loop manner. In MRAS method a reference model is constructed which estimates some variable  $x_d$ ,  $x_q$  (e.g rotor flux linkage component  $\psi_{dr}$  and  $\psi_{qr}$  or back emf components,  $e_{md}$ ,  $e_{mq}$  or reactive power

etc.). Same state variables are estimated from another model called adaptive model which then compared to create an error vector to feed an adjustable method. The adjustable method gives the estimated speed which drives adaptive model to minimise the error vector created by this two model. Most important part of MRAS is to design of adaptation mechanism. For designing adaptive mechanism of a MRAS, system has to follow Popov's criteria of hyperstability which gives stability and quick response of the system.

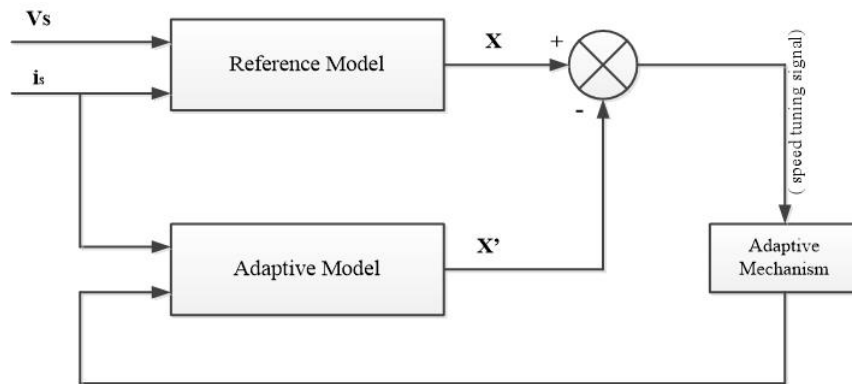


FIGURE 1.2: MRAS Based Speed Estimation Scheme

## 1.5 ORGANISATION OF THE REPORT

**chapter1** includes state-of art and potential application of vector controlled induction motor drive. It also covers vector control techniques applied to squirrel cage induction motor and tells about the requirement, objectives, and methods of vector control.

**Chapter2** deals with an exhaustive literature review on the vector controlled induction motor drive. It includes state of art method of estimation of speed by sensing the winding currents and DC link voltage.

**Chapter3** explains briefly the modelling and MATLAB implementation of the vector controlled induction motor drive (VCIMD).

**Chapter4** discusses about the design and modelling of the speed estimation schemes of motor, used along with its basic operation.

**Chapter5** displays the results obtained in simulation of the 2hp and 30hp motor under different operating conditions in Matlab/Simulink environment.

Finally, it is followed by Conclusions and Bibliography which can be used for further reading. Appendixes are also added after Bibliography where appendix-I provides various machine parameters used for simulation in Matlab/Simulink and appendix-II shows a list of PI controller values used in different speed estimation schemes.

## Chapter 2

# LITERATURE REVIEW

---

### 2.1 INTRODUCTION

The preceding chapter deals with a general overview of the vector control techniques, various potential applications and the state of the art as applied to three-phase squirrel cage induction motor. The present chapter covers a literature review relating to various developments in vector control techniques. It includes a review of closed loop speed controlled induction motor drives and various methods to eliminate speed sensor from the drive system to reduce the system cost.

### 2.2 SIGNIFICANT DEVELOPMENTS

From the available literature it is revealed that the method of vector control has become a major tool for squirrel cage induction motor to provide its dynamic performance equivalent to compensated separately excited dc motor. The popularity of vector control has been established on the advantages of vector control over scalar control techniques [1-6].

The squirrel cage induction motor has many advantages over dc motor in comparison with size, inertia, efficiency, reliability, cost, power to weight ratio and robust rotor etc. The main advantage with separately excited dc motor is the ease of control and better



dynamic performance. The popularity of vector control has been established on the advantages of vector control over scalar control techniques [7–9].

A number of software packages for simulation have been proposed in recent years. For electronic circuits like SPICE and SABER, power networks like the EMTP and EUROSTAG or specialized simulation of power electronics such as SIMPLORO, POSTMAC, SIMSEN, ANSIM and PSCAD. Dedicated simulation softwares like MATLAB with Simulink and power-system block set (PSB) toolboxes have made the modelling and simulation of such system efficient and simple [10]. Elimination of sensor has provided the reduction of overall cost of the drive [11–18].

## 2.3 LITERATURE REVIEW

In the last three decades, the vector control (VC) technique also known as field-oriented Control (FOC) technique employed to control three phase squirrel cage induction motors [1, 6, 19–21] has been dealt with in great detail in the literature. Before the advent of vector control technique for induction motors, various other control methods e.g voltage control, frequency control, rotor resistance control, v/f control [2, 6], flux control [6, 19] was existed. Such control techniques result in satisfactory response only in steady state conditions. Blashke [10] has reported the pioneer concept to initiate the work based on the concept of vector control. Vector control is control technique which is used to decouple control between flux and torque in an induction motor similar to a separately excited DC motor. Y.S Lai et al [22] has discussed the development of sensorless vector controllers based on stator flux oriented control (SFOC) and rotor flux oriented control. Because of several advantages sensorless speed drive keeps on maturing through yours as revealed in [10, 21, 23–25]. The problem of sensorless speed drive and an approach of solving problems is well documented in [26]. Xu and Novotony [27] have reported the estimation of synchronous speed from stator flux. The rotor speed is estimated from the difference between synchronous speed and estimated slip speed. Chin [14] has proposed various issues involved in making an estimation of rotor speed. Shine et al [17] have discussed on the aspect of achieving accuracy in flux calculation.

The speed estimation involves scheme based on Model Reference Adaptive System (MRAS) has employed the comparison of out of the two estimators- one being the reference model and other being adjustable model [23, 28–30]. Colin Schauder [15] has

described the model reference adaptive system for estimation of rotor speed using terminal voltages and currents with rotor flux as a functional candidate. Recently various modification of MRAS been done all are summarized in [31]. Back emf based MRAS is presented in [32] where Peng and Fukao have also shown estimation of speed using air-gap reactive power as a functional candidate. A comparative study in [33] is been done between Rotor Flux(RF) based and Back-Emf based MRAS whereas [34] has shown a simulation work on the basis of dynamic performance of the two methods. Stability of back emf based MRAS is documented in great detail in [35]. The approach is independent of the value of stator resistance and thermal variations in its value. Because of unstable nature of airgap power based MRAS in regenerative mode of operation an instantaneous terminal reactive power based MRAS is proposed in [36],[37]. Another reactive power based MRAS using instantaneous reactive power in reference model and steady state reactive power is presented in [38],[39]. Further improvement in reactive power based improvement is discussed in [40, 41]. Recently an approach for designing RF-based MRAS based on Liapunov theorem has been introduced in [42].

Luenberger speed observer [43, 44] schemes are based on the estimation of rotor flux through one observer and the speed is derived by the stator current error and the estimated rotor flux. Schemes adopting observers can be treated as MRAS as well, wherein the motor is considered as the reference model and the observer can be taken as adaptive model. Extended Kalman filter [45, 46] is another adaptive filter which is also used for sensorless speed estimation. Yang and chin [11] have estimated speed with an observer. To make the estimation accurate at low speeds, the stator resistance is also identified simultaneously. The drive is operated in a wide range of speed especially at low speed. In [20, 47] speed estimation is done using a flux model based observer which uses terminal conditions of the motor and its parameters and it eliminates the use of speed sensor. A simple technique to estimate the rotor speed is derived in [16, 48]. Speed estimation on the basis of the difference between two flux estimators is shown in [49]. Its convergence performance is being analyzed and a novel pole assignment method is proposed. [50] proposes a simple method to accurately estimate the stator flux vector and demonstrate its functioning operation at very small angular velocities in every sampling period. Dybkowski et al. in [51] have shown a method to implement a speed sensorless induction motor drive with magnetizing reactance estimation. A sensorless scheme using adaptive neural-fuzzy inference system is reported in [52].

## Chapter 3

# MATHEMATICAL MODELING OF VECTOR CONTROLLED INDUCTION MOTOR DRIVE

---

### 3.1 SPEED CONTROLLER

Error created by reference speed ( $\omega^*$ ) and motor shaft speed ( $\omega_r$ ) is used to drive the speed controller which is essential for a vector control drive. The speed controller may be of different types depending upon the required dynamic performance of the drive. Here a PI controller is used as a speed controller. The output of speed controller is command torque ( $T^*$ ) which is input to the limiter.

### 3.2 LIMITER

The limiter puts a limit on the output of the speed controller and output is considered as reference torque ( $T^*$ ). Limit on torque ( $T$ ) is required since during transients (such as starting, speed reversal, loading) experienced by the drive, the output of the speed controller jumps quickly to a very high value which may go beyond the breakdown torque limit of the drive causing instability and over current. This is because the reference torque ( $T^*$ ) effects the reference value of the torque producing component of the stator

current ( $i_{qs}^*$ ). Therefore, in order to operate the drive in safe region with safe operating current putting a limit on the command output is necessary. This limit ensures that in no case the inverter output current jumps more than a set value thereby providing the feature of inherent over current protection in the drive.

When an abnormality arises because of the step changes in speed or load on the motor shaft the reference torque which is command signal at the output of the limiter gets saturated at its maximum value with an appropriate polarity. Depending upon the desired direction of rotation of the motor. With this limit on the command torque ( $T^*$ ), it is ensured that in no case the current crosses a set limit for breakdown torque. This provides inherent stability to the drive.

### 3.3 FIELD WEAKENING CONTROL

Field weakening in the vector control drive is analogous to field control of a separately excited DC motor. Field weakening is normally used to operate above base speed. Below base speed a constant flux is maintained to realize a constant torque drive while above base speed constant power drive is obtained. The reference value of the exciting current ( $i_{mr}^*$ ) is a function of the rotor speed. Mathematically, the logic for the exciting current may be stated as follows:

$$i_{mr}^* = I_m \quad \text{if } \omega_r < \text{base speed} \quad (3.1)$$

$$i_{mr}^* = \frac{k_f \times I_m}{\omega_r} \quad \text{if } \omega_r > \text{base speed} \quad (3.2)$$

Where  $k_f$  is flux constant and  $I_m$  is rms value of the magnetizing current.

### 3.4 VECTOR CONTROL STRUCTURE

To perform vector control, following steps are to be followed:

- Measure the motor quantities (e.g phase currents)
- Calculate the rotor flux space vector magnitude and position angle
- Transform  $i_{qs}^*$  and  $i_{ds}^*$  into  $i_{as}^*, i_{bs}^*$  and  $i_{cs}^*$
- Compare  $i_{as}^*, i_{bs}^*$  and  $i_{cs}^*$  with actual currents and generate pwm.

The output of the speed loop, reference torque ( $T^*$ ), is processed in the vector controller along with reference magnetizing current vector ( $i_{mr}^*$ ). The vector controller computes the orthogonal current components ( $i_{qs}^*$  and  $i_{ds}^*$ ) of the stator current vector. The currents ( $i_{qs}^*$  and  $i_{ds}^*$ ) being in synchronously rotating reference frame are dc quantities in nature. In order to vector control of induction motor, its stator currents are controlled in such a way that orthogonal currents ( $i_{qs}$  and  $i_{ds}$ ) and flowing through the stator winding have one to one correspondence with these reference orthogonal current components ( $i_{qs}^*$  and  $i_{ds}^*$ ). For coordinate transformation the vector controller should have knowledge about rotor flux position which is estimated by integrating the sum of rotor speed ( $\omega_r$ ) and command slip ( $\omega_{sl}^*$ ). The quantity so obtained gives flux angle ( $\theta$ ) in radians.

### 3.4.1 Modeling of Vector Controller

Vector controller can be realized by the following equations

$$i_{ds}^* = i_{mr} + \tau_r \frac{d}{dt} i_{mr} \quad (3.3)$$

$$i_{qs}^* = \frac{T^*}{k i_{mr}^*} \quad (3.4)$$

$$\omega_{sl}^* = \frac{i_{qs}^*}{T_r i_{mr}^*} \quad (3.5)$$

$$k = \frac{3}{2} \left( \frac{P}{2} \right) \frac{M}{1 + \sigma_r}$$

Where  $i_{ds}^*$  and  $i_{qs}^*$  refer to the flux and torque producing components of the stator current space vector at  $n_{th}$  instant respectively,  $\omega_{sl}^*$  refers to the  $n_{th}$  instant reference slip speed.  $P$ ,  $M$ ,  $\sigma_r$  are the number of poles, mutual inductance and rotor leakage factor respectively. In addition to the decoupled components of the stator current space vector, the flux angle is defined at  $n_{th}$  instant as:

$$\theta(n) = \theta(n-1) + (\omega_{sl} + \omega_r) \Delta T \quad (3.6)$$

Where  $\theta(n)$  is the value of flux angle at the  $n_{th}$  instant,  $\theta(n-1)$  is the value of the flux at the  $(n-1)_{th}$  instant.  $\omega_{sl}^*$ ,  $\omega_r$  and  $\Delta T$  are the reference slip, frequency, rotor speed and sampling time respectively.

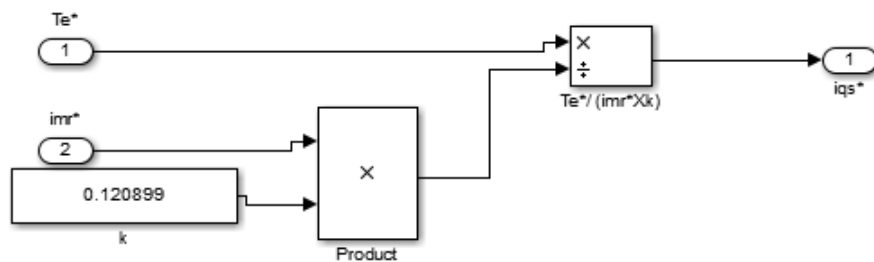


FIGURE 3.1: Vector Controller Subsystem(A)

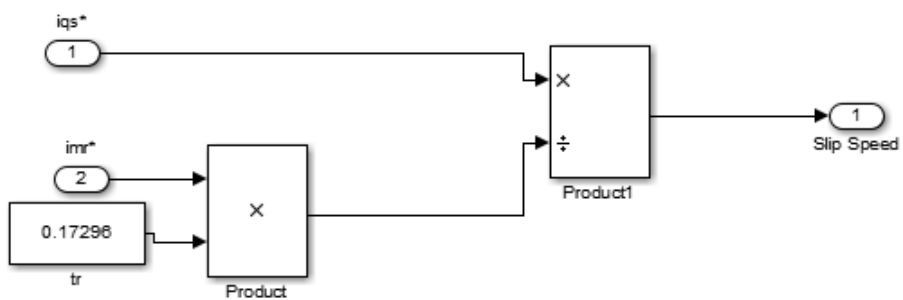


FIGURE 3.2: Vector Controller Subsystem(B)

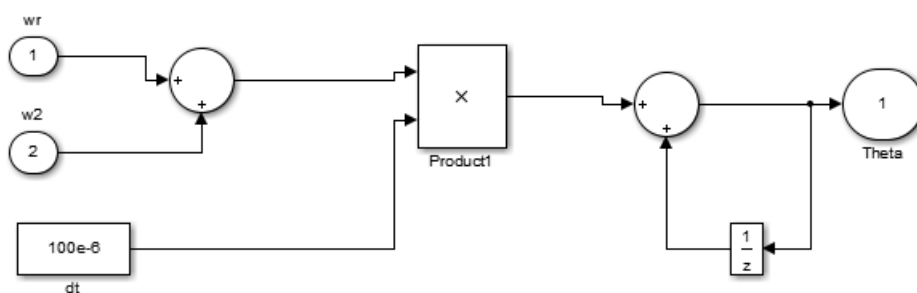


FIGURE 3.3: Vector Controller Subsystem(C)

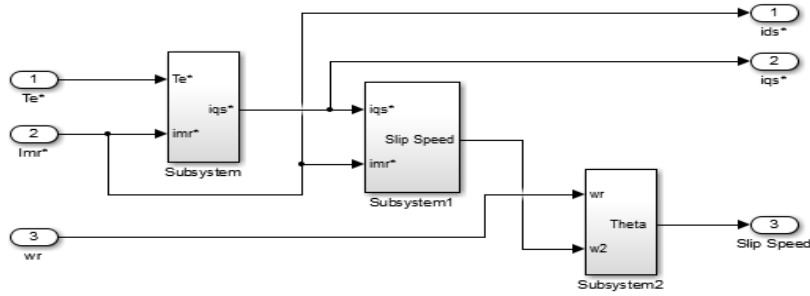


FIGURE 3.4: Vector Controller

### 3.5 INVERSE CLARKE'S AND PARK'S TRANSFORMATION

The modeling is based on the following: equations:

$$i_{bs}^* = \frac{1}{2} [i_{ds}^* (-\cos(\rho) + \sqrt{3}\sin(\rho))] + i_{qs}^* (\sin(\rho) + \sqrt{3}\cos(\rho)) \quad (3.7)$$

$$i_{as}^* = -i_{qs}^* \sin(\rho) + i_{ds}^* \cos(\rho) \quad (3.8)$$

$$i_{cs}^* = -(i_{as}^* + i_{bs}^*) \quad (3.9)$$

Where  $i_{ds}^*$ ,  $i_{qs}^*$  refer to the decoupled component of the stator current space vector  $i_s^*$  and  $i_{as}^*$ ,  $i_{bs}^*$  and  $i_{cs}^*$  refer to the three phase reference currents in stationary reference frame.

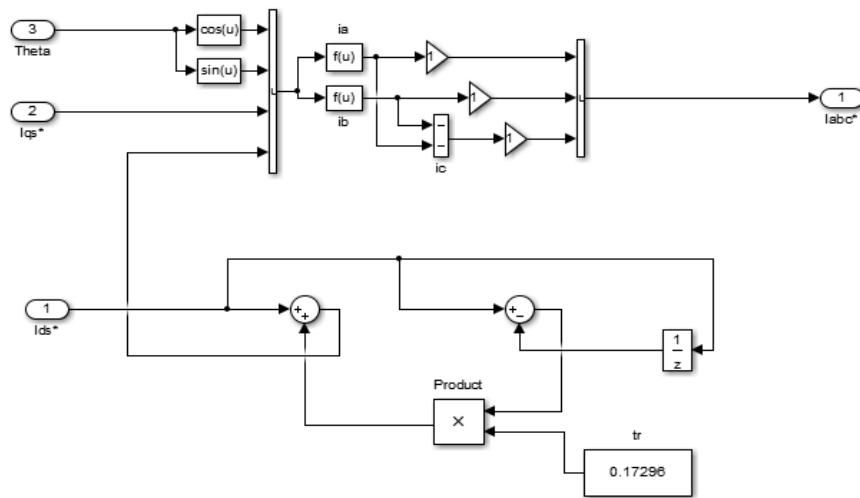


FIGURE 3.5: Two Phase Rotating Frame to Three Phase Stationary Frame Converter

### 3.6 CURRENT CONTROLLER

In order to ensure that the three phase currents flowing through the motor windings, follow the three phase currents, a suitable current controller is used. For this purpose a variable frequency inverter is employed along with a current controller. For maintaining the motor currents in such a way that they vary in a definite manner the inverter requires a particular type of ON/OFF (pwm) pattern for its switches (an IGBT with anti-parallel diode). The current controller is responsible for generating desired switching pattern and is generally of two types one is sine pwm current controller while the other one is Hysteresis current controller. The current controller compares the winding currents for generating desired switching pattern. The current controller compares the winding currents ( $i_{as}, i_{bs}, i_{cs}$ ) with the reference currents ( $i_{as}^*, i_{bs}^*, i_{cs}^*$ ). As a result of this comparison a switching pattern is obtained which controls ON/OFF time of inverter switches.

#### 3.6.1 Modeling of Pulse Width Modulated(PWM) Current Controller (CC)

The PWM-CC compares the sensed winding currents  $i_{as}, i_{bs}$  and  $i_{cs}$  with their reference values  $i_{as}^*, i_{bs}^*$  and  $i_{cs}^*$  and evaluates the current error. This signal is amplified by a simple gain factor and compared with a high frequency triangular wave carrier signal, with a frequency  $f_s$  of the inverter.

Based on the comparison of modulating signal and switching frequency triangular carrier wave, combination of switching functions for three phases are decided. The current is as:

$$\begin{aligned}
 i_{ase} &= i_{as}^* - i_{bs}, & i_{bse} &= i_{bs}^* - i_{bs}, & i_{cse} &= i_{cs}^* - i_{cs}, \\
 \text{if } ki_{ase} > y(t) & \text{ then } SF_a = 1 \text{ else } SF_a = 0. \\
 \text{if } ki_{bse} > y(t) & \text{ then } SF_b = 1 \text{ else } SF_b = 0. \\
 \text{if } ki_{cse} > y(t) & \text{ then } SF_c = 1 \text{ else } SF_c = 0.
 \end{aligned}$$

Where  $y(t)$  refers to the instantaneous value of triangular carrier wave with K being the gain of Proportional controller.



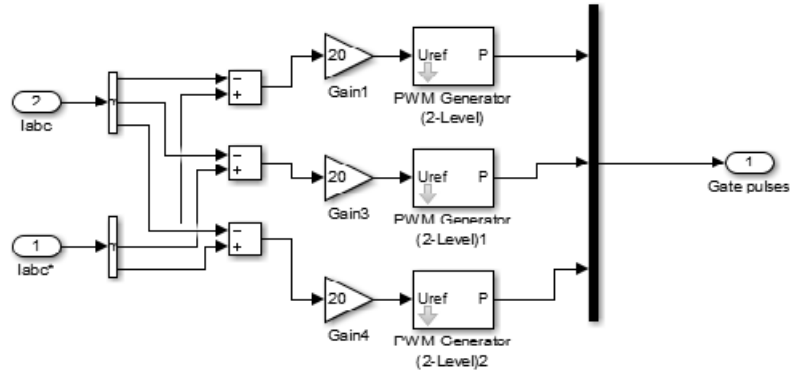


FIGURE 3.6: PWM Generator

### 3.7 CURRENT CONTROLLED VOLTAGE SOURCE INVERTER

The current controlled voltage source inverter which gets its switching signals from the current controller, maintains the motor winding currents in a manner which conforms to the need of vector control. It has a constant voltage source at its input and gives three phase PWM voltage and frequency. These in turn depend upon the set speed of the drive and different operating conditions being encountered by the drive such as starting, speed reversal and also smooth running of the drive in any quadrant of torque speed characteristics.

#### 3.7.1 Modeling of Voltage Source Inverter(VSI)

The switching function  $SF_a$ ,  $SF_b$  and  $SF_c$  determines ac output voltage of the inverter. Switching functions are received from the sinusoidal pwm current controller.

The magnitude of three voltages can be mathematically expressed as:

$$v_{as} = \frac{v_{dc}(2SF_a - SF_b - SF_c)}{3} \quad (3.10)$$

$$v_{bs} = \frac{v_{dc}(2SF_b - SF_a - SF_c)}{3} \quad (3.11)$$

$$v_{cs} = \frac{v_{dc}(2SF_c - SF_b - SF_a)}{3} \quad (3.12)$$

Where  $v_{as}$ ,  $v_{bs}$  and  $v_{cs}$  are the per phase voltages respectively.

## 3.8 INDUCTION MOTOR

It is assumed that we work on star-connected ac induction motor with cage construction. Depending upon the set value  $\omega_r$  it rotates at a particular speed and converts the electrical energy into useful mechanical energy.

### 3.8.1 Modeling of Induction Motor

Modelling of induction motor is done using  $\alpha$ - $\beta$  reference frame. The voltage current relationship in the stationary frame of the induction motor in terms of  $\alpha$ - $\beta$  is expressed as:

$$[i] = [i_{\alpha s}, i_{\beta s}, i_{\alpha r}, i_{\beta r}]$$

$$[v] = [v_{\alpha s}, v_{\beta s}, v_{\alpha r}, v_{\beta r}]$$

In the above equation  $v_{\alpha s}$  and  $v_{\beta s}$  are the forcing functions impressed across the stator windings.  $v_{\alpha r}$  and  $v_{\beta r}$  are zero in case of three-phase squirrel cage induction motor.

$$v_{\alpha s} = v_{as} \quad (3.13)$$

and

$$v_{\beta s} = \frac{(v_{bs} - v_{cs})}{\sqrt{3}} \quad (3.14)$$

$[R]$ ,  $[L]$  and  $[G]$  are referred as resistance, inductance and rotational inductance matrix respectively.  $\alpha, \beta, s$  and  $r$  represent the direct axis, quadrature axis, stator quantities and rotor quantities respectively.

The derivative of rotor speed is obtained from the torque balance equation as follows:

$$p\omega_r = \left(\frac{p}{2}\right) \left[\frac{T_e - T_l}{J}\right] \quad (3.15)$$

$T_l$  refers to the load torque on the motor shaft, which includes friction and windage torque and  $T_e$  refers to the electromagnetic torque developed by motor as defined:

$$T_e = \left(\frac{3}{2}\right) \left(\frac{p}{2}\right) L_m (i_{qs}i_{dr} - i_{ds}i_{qr}) \quad (3.16)$$

## Chapter 4

# SPEED ESTIMATION SCHEMES

---

### 4.1 OPEN LOOP SPEED ESTIMATOR

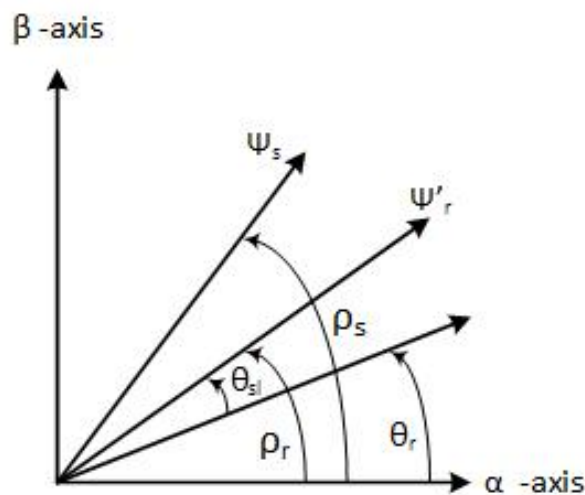


FIGURE 4.1: Vector Diagram of Relevant Phasors

In this scheme speed of rotor flux space vector ( $\psi_r$ ) is used to estimate rotor speed. For that, it requires the accurate estimation of slip speed  $\omega_{sl}$ . Here stator voltages ( $v_{\alpha s}$ ) and  $v_{\beta s}$  are not monitored rather they are reconstructed from monitored dc link voltage and switching states of the inverter as described earlier in 3.10 to 3.12. Figure 4.1 shows the rotor flux linkage space phasor, the position of which is used in developing rotor

speed of this scheme. From the reconstructed stator voltages, stator flux can be derived from voltage model of IM in stationary reference frame. This requires the knowledge of stator resistance ( $R_s$ ), the direct and quadrature axis components of currents ( $i_{\alpha s}$  and  $i_{\beta s}$ ). The rotor flux ( $\psi_r$ ) can be obtained from stator flux ( $\psi_s$ ) with knowledge of motor parameters ( $R_s, L_m, L_r, L_s$ ). From this estimated value of rotor flux, rotor speed can be evaluated.

#### 4.1.1 CALCULATION OF SPEED

The speed estimation can be broken in two steps:

##### 4.1.1.1 Calculation of Rotor Flux ( $\psi_{\alpha r}$ and $\psi_{\beta r}$ )

The voltage model of IM can be described in stationary reference frame as follows

$$v_{\alpha s} = R_s i_{\alpha s} + \frac{d\psi_{\alpha s}}{dt} \quad (4.1)$$

$$v_{\beta s} = R_s i_{\beta s} + \frac{d\psi_{\beta s}}{dt} \quad (4.2)$$

By rearranging above equations stator flux linkage can be expressed as

$$\psi_{\alpha s} = \int (v_{\alpha s} - R_s i_{\alpha s}) dt \quad (4.3)$$

$$\psi_{\beta s} = \int (v_{\beta s} - R_s i_{\beta s}) dt \quad (4.4)$$

also in stationary reference frame

$$\psi_{\alpha s} = \frac{L_r}{L_m} (\psi_{\alpha s} - L_s i_{\alpha s}) \quad (4.5)$$

And

$$\psi_{\beta s} = \frac{L_r}{L_m} (\psi_{\beta s} - L_s i_{\beta s}) \quad (4.6)$$

##### 4.1.1.2 Calculation of Angular Rotor-Slip Speed ( $\omega_{sl}$ )

It is possible to implement an angular rotor-slip speed estimator ( $\omega_{sl}$ ) by considering the rotor voltage equation of the induction motor. If the rotor voltage equation is expressed

in the rotor-flux oriented reference frame, then

$$0 = R_r i_{dr} + p\psi_{dr} - \omega_{sl}\psi_{qr} \quad (4.7)$$

$$0 = R_r i_{qr} + p\psi_{qr} + \omega_{sl}\psi_{dr} \quad (4.8)$$

And

$$\psi_{dr} = L_r i_{dr} + L_m i_{ds} \quad (4.9)$$

$$\psi_{qr} = L_r i_{qr} + L_m i_{qs} \quad (4.10)$$

Now taking the direct axis of the reference frame along the rotor flux linkage we get  $\psi_{qr} = 0$  and  $\psi_{dr} = \psi_r$ . Now using equations 4.7 to 4.10 and above conditions

$$i_{ds} = \frac{1}{L_m}(1 + T_r p)\psi_r \quad (4.11)$$

And

$$\omega_{sl} = \frac{L_m i_{qs}}{\psi_r T_r} \quad (4.12)$$

Also, for frame aligned with rotor flux linkage,

$$\begin{bmatrix} i_{qs} \\ i_{ds} \end{bmatrix} = \begin{bmatrix} \cos\rho_r & \sin\rho_r \\ -\sin\rho_r & \cos\rho_r \end{bmatrix} \begin{bmatrix} i_{\beta s} \\ i_{\alpha s} \end{bmatrix} \quad (4.13)$$

If the expression of  $i_{qs}$  from above transformation matrix is substituted in the equation 4.12 then

$$\omega_{sl} = \frac{-i_{ds}\sin\rho_r + i_{qs}\cos\rho_r}{T_r\psi_r} \quad (4.14)$$

where  $\rho_r$  is the angle of rotor flux with respect to the real axis of the stationary reference frame. By considering  $\sin\rho_r = \frac{\psi_{qr}}{\psi_r}$  and  $\cos\rho_r = \frac{\psi_{dr}}{\psi_r}$ ,  $\omega_{sl}$  can be written as

$$\omega_{sl} = \frac{L_m(-\psi_{qr}i_{ds} + \psi_{dr}i_{qs})}{T_r\psi_r^2} \quad (4.15)$$

Where  $\psi_{qr}$  and  $\psi_{dr}$  are rotor flux linkages in the stationary reference frame. Above equation can be used to monitor the angular slip frequency by monitoring the stator currents, and also by using the rotor flux linkages. It is possible to obtain an expression for the

motor speed by considering that

$$\omega_r = \omega_e - \omega_{sl} \quad (4.16)$$

Where  $\omega_r$  is the rotor speed and  $\omega_e = \frac{d\rho}{dt}$  is the speed of the rotor flux in stationary reference, and  $\omega_{sl}$  is the angular slip speed.

Now  $\rho_r = \tan^{-1}\left(\frac{\psi_{\beta s}}{\psi_{\alpha s}}\right)$  and it follows that  $\omega_e = \frac{d \tan^{-1}\left(\frac{\psi_{\beta s}}{\psi_{\alpha s}}\right)}{dt}$

Finally using equation 4.16 rotor speed becomes

$$\omega_r = \frac{d \tan^{-1}\left(\frac{\psi_{\beta s}}{\psi_{\alpha s}}\right)}{dt} - \frac{L_m(-\psi_{qr}i_{ds} + \psi_{dr}i_{qs})}{T_r \psi_r^2} \quad (4.17)$$

A rotor speed estimator is hence constructed which uses the monitored stator currents and the rotor flux components, which, however, can be obtained from the stator flux linkages as discussed above. The accuracy of such a speed estimator depends greatly on the machine parameter used, and also on the model used for the estimation of the rotor flux-linkage components. A possible implementation is shown in figure 4.2. This contains the following three machine parameters:  $R_s, L_m$  and  $k = \frac{L_m}{L_r}$ .

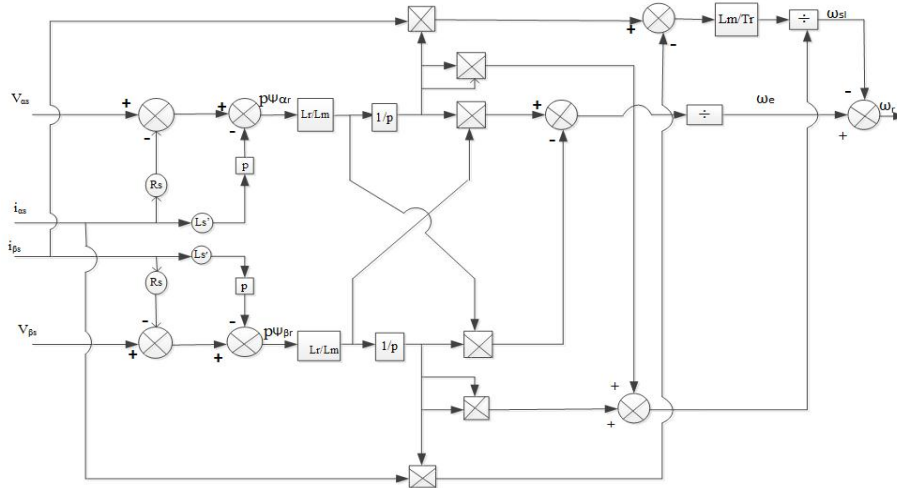


FIGURE 4.2: Block Diagram of Open Loop Speed Estimator

### 4.1.2 Simulation Block of Open Loop Speed Estimator

The speed estimator block is now described in figures 4.3 which shows the flux calculator subsystem based on the discussion in section 5.2. The rotor flux components thus estimated are then used in the calculation of rotor speed using the scheme discussed

above. Figure 4.4 shows the block diagram for the speed estimator subsystem used in modelling of the proposed Sensorless drive in Simulink/Matlab environment. The speed estimator block uses the mean or average calculator to suppress the high frequency noise developed in estimated speed. This noise is due to differentiation operation of estimated speed.

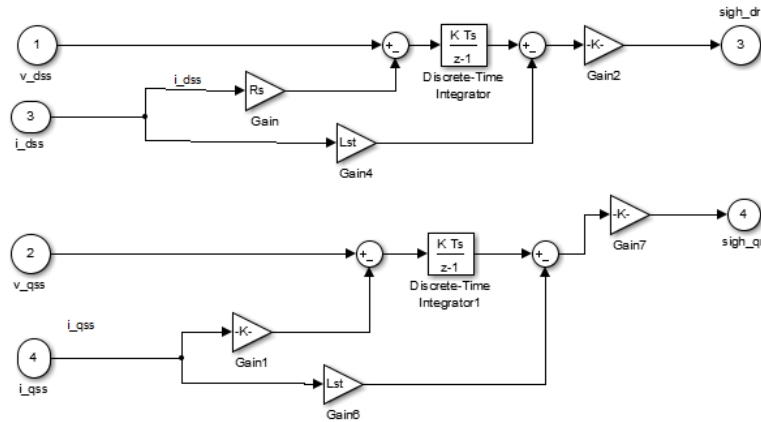


FIGURE 4.3: Simulink Block Diagram for Flux Calculator Used in Speed Estimator Block

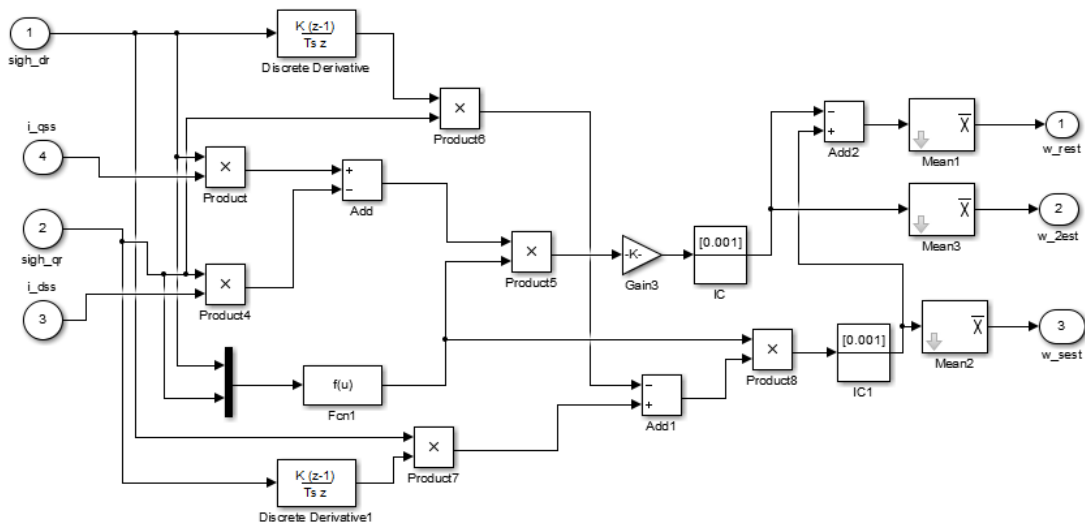


FIGURE 4.4: Simulink Block Diagram For Speed Estimation

## 4.2 MRAS BASED SPEED ESTIMATOR

There are many techniques have been suggested by researchers in literature for estimation of speed in sensorless way. Among them MRAS (Model reference adaptive system) based method is very popular as it is computationally less intensive and shows straight forward approach in terms of stability . MRAS basically consists of a Reference model and an adaptive model where both the models compute same quantity, and at the same

time reference model is free from the quantity which is to be estimated whereas adaptive model is involved with the quantity which is being estimated. Now comparing the outputs of the two models an error vector is created which is used to tune an adaptive law to give estimate quantity.

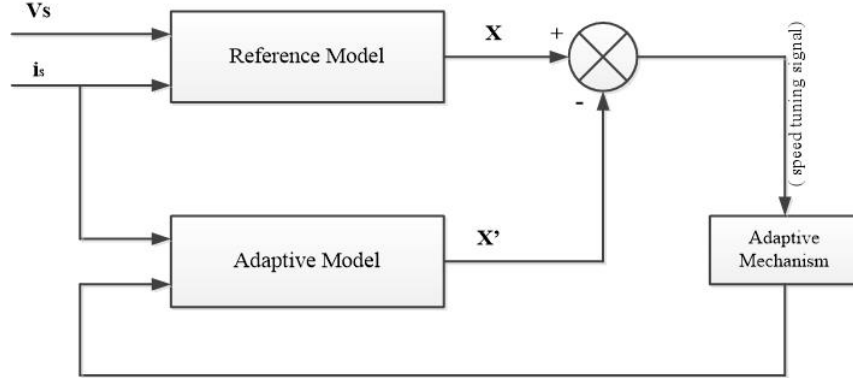


FIGURE 4.5: MRAS Based Speed Estimation Scheme

Depending upon the type of tuning signal generated, from the two models, a number of MRAS based speed estimation schemes can be realized such as rotor flux based, back emf based, airgap-reactive power based MRAS and artificial neural network based MRAS. Here the performance of the rotor flux based MRAS , back-emf based MRAS and reactive power based MRAS is studied for speed estimation.

### 4.2.1 Rotor flux based MRAS

In this type of MRAS both RF and AM model compute rotor flux. Then the error of these two rotor flux vector is fed to a PI controller, whose output is taken as speed.

#### 4.2.1.1 Reference Model

$$\psi_{\alpha r} = \frac{L_r}{L_m} \left[ \int (v_{\alpha s} - R_s i_{\alpha s}) - \sigma L_s i_{\alpha s} \right] \quad (4.18)$$

$$\psi_{\beta r} = \frac{L_r}{L_m} \left[ \int (v_{\beta s} - R_s i_{\beta s}) - \sigma L_s i_{\beta s} \right] \quad (4.19)$$

#### 4.2.1.2 Adaptive Model

$$\psi_{\alpha r} = \int \left( \frac{1}{T_r} \psi_{\alpha r} - \omega_r \psi_{\beta r} + \frac{L_m}{T_r} i_{\alpha s} \right) \quad (4.20)$$



$$\psi_{\beta r} = \int \left( \frac{1}{T_r} \psi_{\beta r} - \omega_r \psi_{\beta r} + \frac{L_m}{T_r} i_{\beta s} \right) \quad (4.21)$$

Speed tuning signal

$$\epsilon = \psi_{\beta r} \hat{\psi}_{\alpha r} - \psi_{\alpha r} \hat{\psi}_{\beta r} \quad (4.22)$$

Estimated speed

$$\omega_r = \left( k_p + \frac{k_i}{s} \right) \epsilon \quad (4.23)$$

Where  $\psi_{\alpha r}, \psi_{\beta r}$  are direct and quadrature axis reference rotor flux in stationary reference frame and  $\hat{\psi}_{\alpha r}, \hat{\psi}_{\beta r}$  are the direct and quadrature axis estimated quantity of rotor flux.

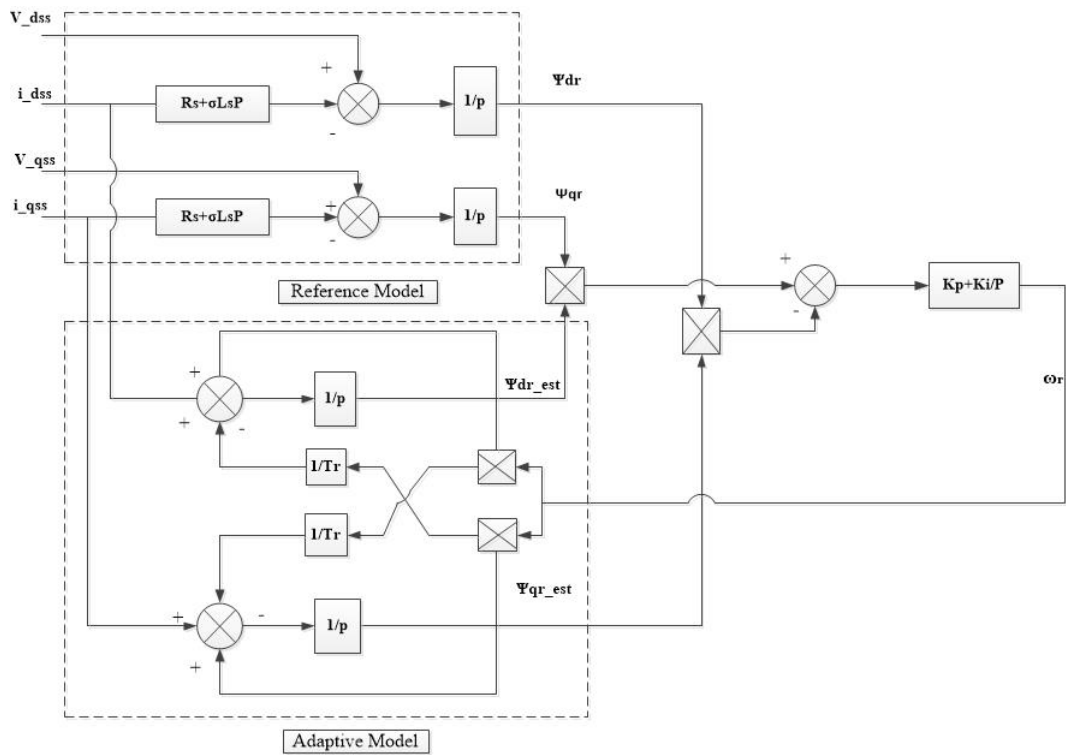


FIGURE 4.6: Block Diagram of RF Based Speed Estimator

### 4.2.1.3 Simulation Block of RF-Based Speed Estimator

In rotor flux based MRAS, rotor flux is used as functional candidate that is why rotor flux is computed from a reference model which is shown in figure 4.7 and from an adaptive model as well shown in figure 4.8. From the figures it is obvious that output of adaptive model depends on rotor speed to be estimated, whereas reference model is completely free from rotor speed.

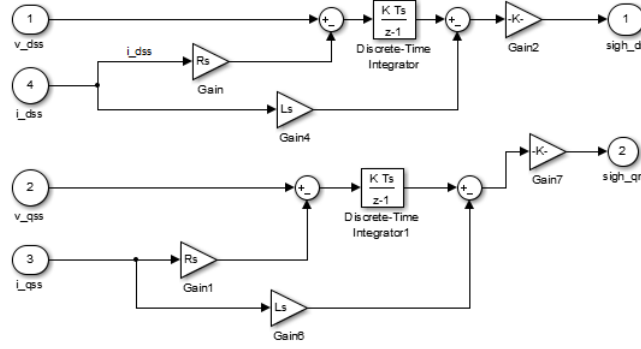


FIGURE 4.7: Simulink Reference model of RF based MRAS

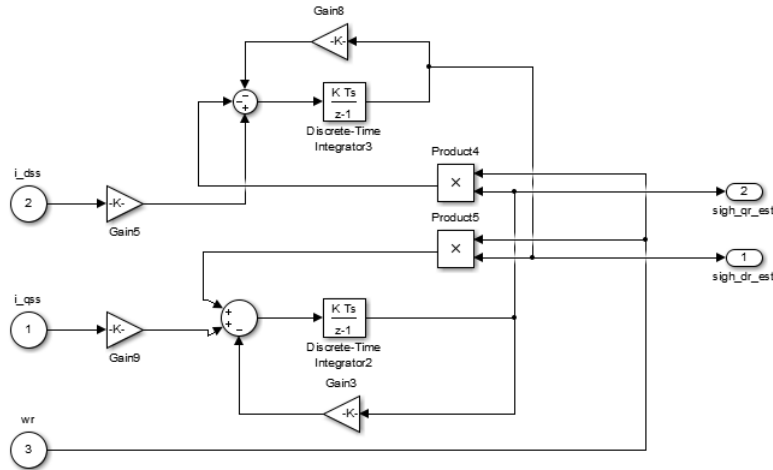


FIGURE 4.8: Simulink Adaptive model of RF based MRAS

## 4.2.2 Back EMF based MRAS

In this method back emf obtained from reference model is compared with back emf of adaptive model which is given to a PI controller where output of this PI controller is the estimated speed.

### 4.2.2.1 Reference Model

$$e_{md} = v_{\alpha s} - \left( R_s i_{\alpha s} + L_s \frac{di_{\alpha s}}{dt} \right) \quad (4.24)$$

$$e_{mq} = v_{\beta s} - \left( R_s i_{\beta s} + L_s \frac{di_{\beta s}}{dt} \right) \quad (4.25)$$

### 4.2.2.2 Adaptive Model

$$\hat{e}_{md} = \frac{L_m}{L_r T_r} (L_m i_{\alpha s} - \psi_{\alpha r} - \omega_r T_r \psi_{\beta r}) \quad (4.26)$$

$$\hat{e}_{mq} = \frac{L_m}{L_r T_r} (L_m i_{\beta s} - \psi_{\beta r} + \omega_r T_r \psi_{\alpha r}) \quad (4.27)$$

Speed tuning signal

$$\epsilon = e_{mq} \hat{e}_{md} - e_{md} \hat{e}_{mq} \quad (4.28)$$

Estimated speed

$$\omega_r = (k_p + \frac{k_i}{s}) \epsilon \quad (4.29)$$

where  $e_{md}, e_{mq}$  are the direct and quadrature axis back emf of reference model in stationary reference and  $\hat{e}_{md}, \hat{e}_{mq}$  are the estimated value of direct and quadrature axis back emf.

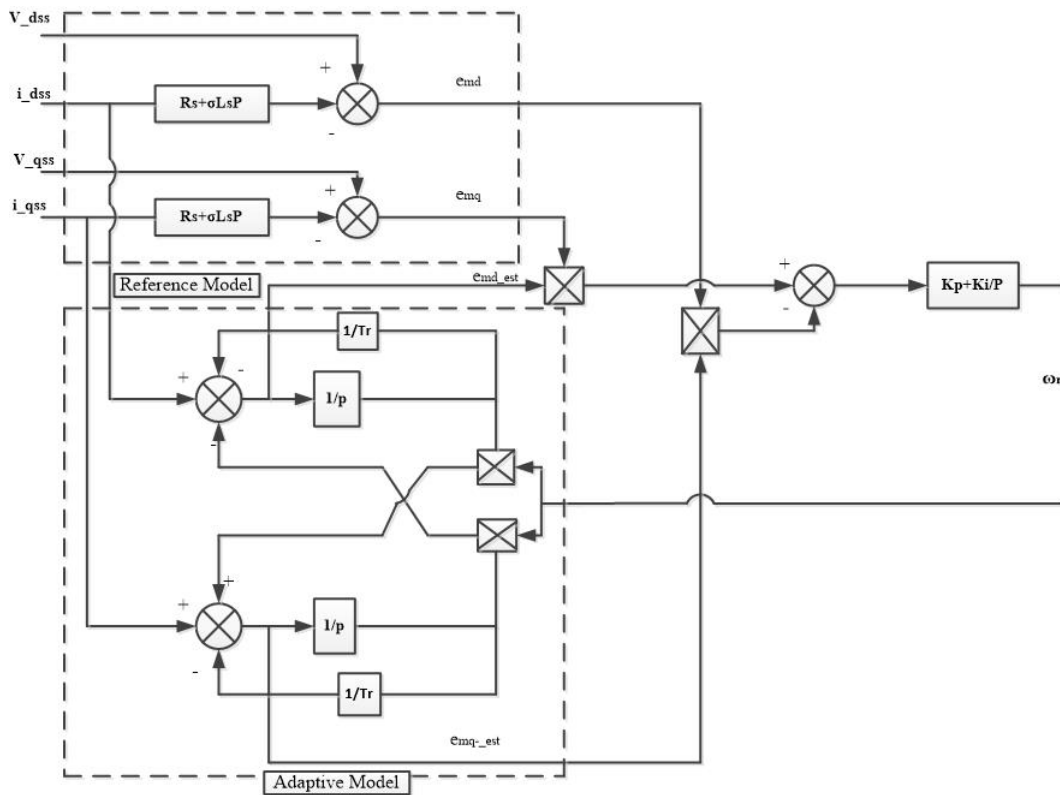


FIGURE 4.9: Block Diagram of back emf Based Speed Estimator

### 4.2.2.3 Simulink Block of Back-Emf Based Speed Estimator

In this MRAS method back emf is used as a functional candidate which is shown in figure 4.10 and figure 4.11 to avoid the problem associated with integrators. As figure 4.10 does not involve the parameter rotor speed, it is used as reference model whereas 4.11 shows the adaptive model.

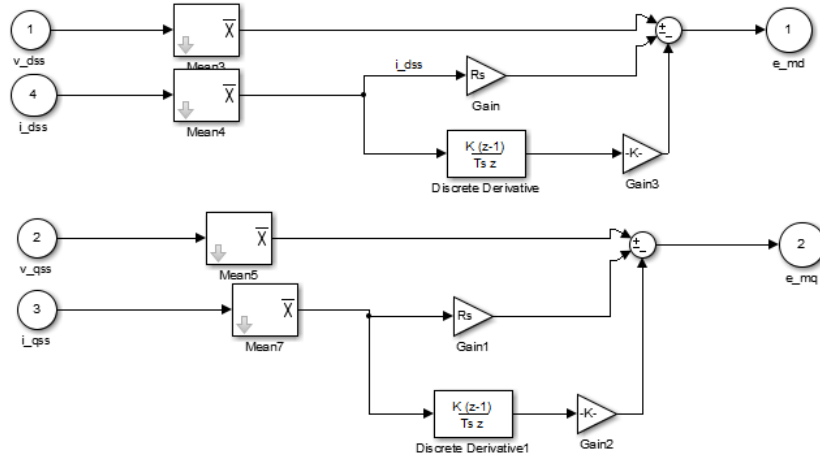


FIGURE 4.10: Simulink reference model of back EMF based MRAS

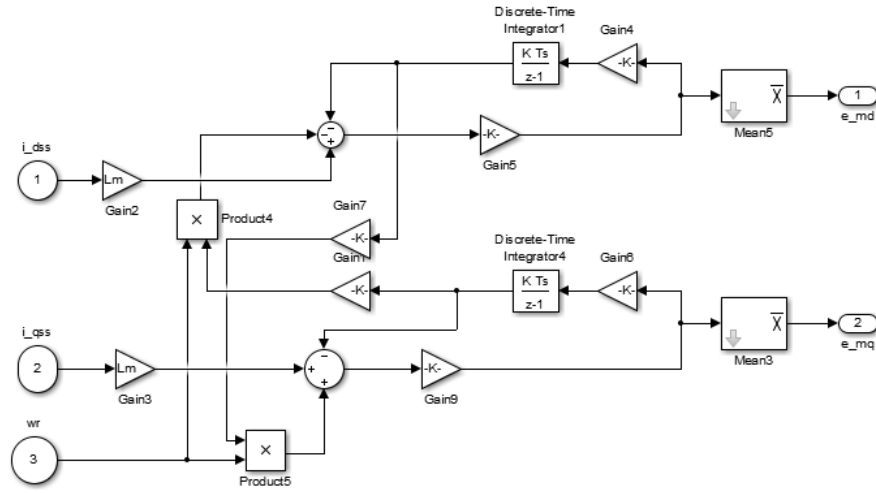


FIGURE 4.11: Simulink Adaptive model of back EMF based MRAS

### 4.2.3 Airgap reactive power based MRAS

Airgap reactive power is used as a functional candidate here to estimate speed. Here also output of reference model is compared with the adaptive model output .the error generated this way is fed to a PI controller which gives desired estimated speed.

#### 4.2.3.1 Reference Model

$$Q_{ref} = e_{mq}i_{\alpha s} - e_{md}i_{\beta s} \tag{4.30}$$

#### 4.2.3.2 Adaptive Model

$$Q_{est} = \hat{e}_{mq}i_{\alpha s} - \hat{e}_{md}i_{\beta s} \tag{4.31}$$

where  $Q_{ref}$  is reference reactive power and  $Q_{est}$  is estimated reactive power and  $e_{md}, e_{mq}, \hat{e}_{md}$  and  $\hat{e}_{mq}$  are described in 4.24, 4.25, 4.26 and 4.27 respectively.

Speed tuning signal

$$\epsilon = Q_{ref} - Q_{est} \tag{4.32}$$

Estimated Speed

$$\omega_r = \left(k_p + \frac{k_i}{s}\right)\epsilon \tag{4.33}$$

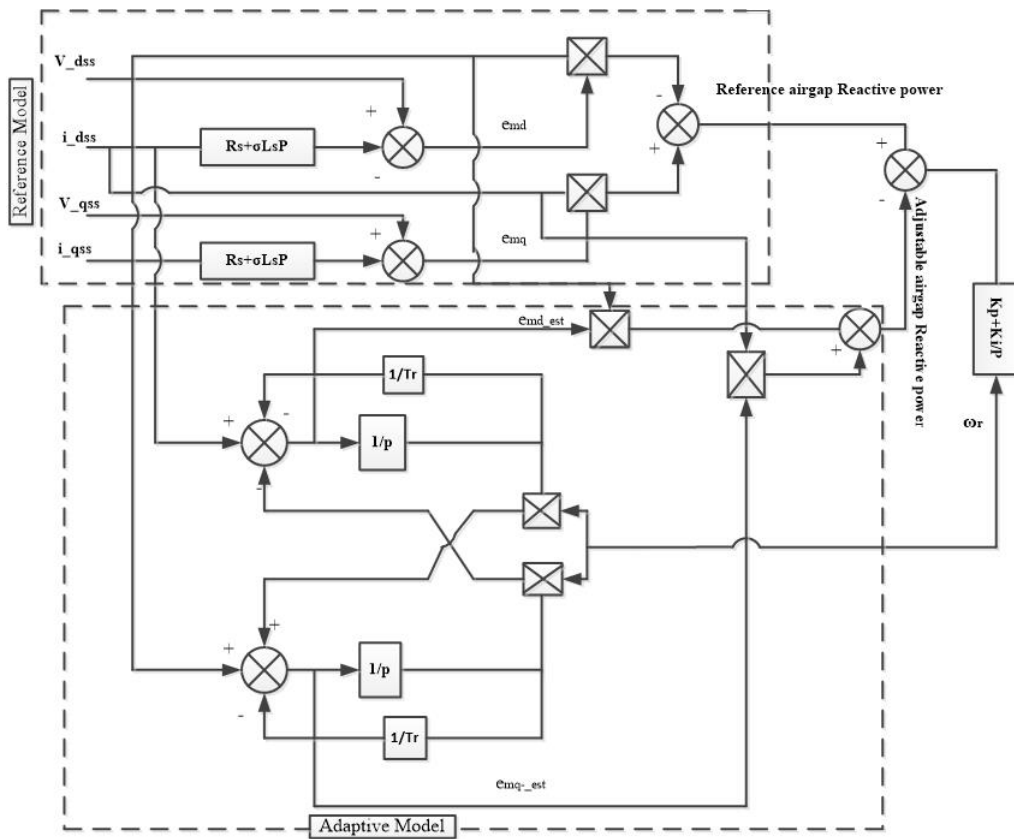


FIGURE 4.12: Block Diagram airgap reactive power based Speed Estimator

### 4.2.3.3 Simulink Block of Airgap Reactive Power Based MRAS

Even though integrator's problem is eliminated in back emf based MRAS but because of its sensitive nature to stator resistance ( $R_s$ ) makes it unusable. To make the speed estimation scheme completely insensitive to stator resistance, airgap power can be used as a functional candidate. Figure 4.13 shows the reference model of this scheme whereas 4.14 is adaptive model as its output depends on rotor speed and it is also obvious that stator resistance is not used to estimate the speed here.

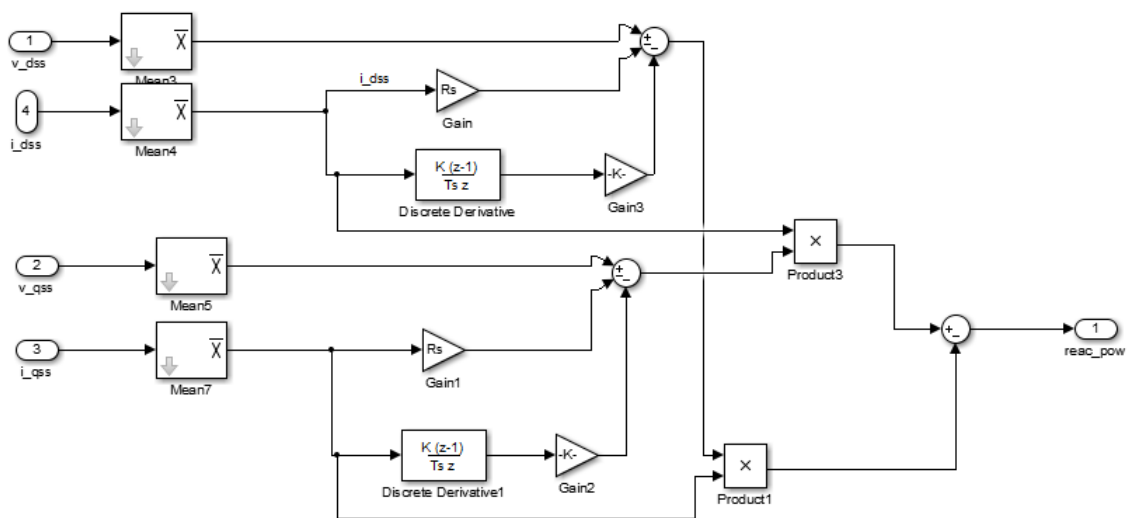


FIGURE 4.13: Simulink Reference model of Airgap power based MRAS

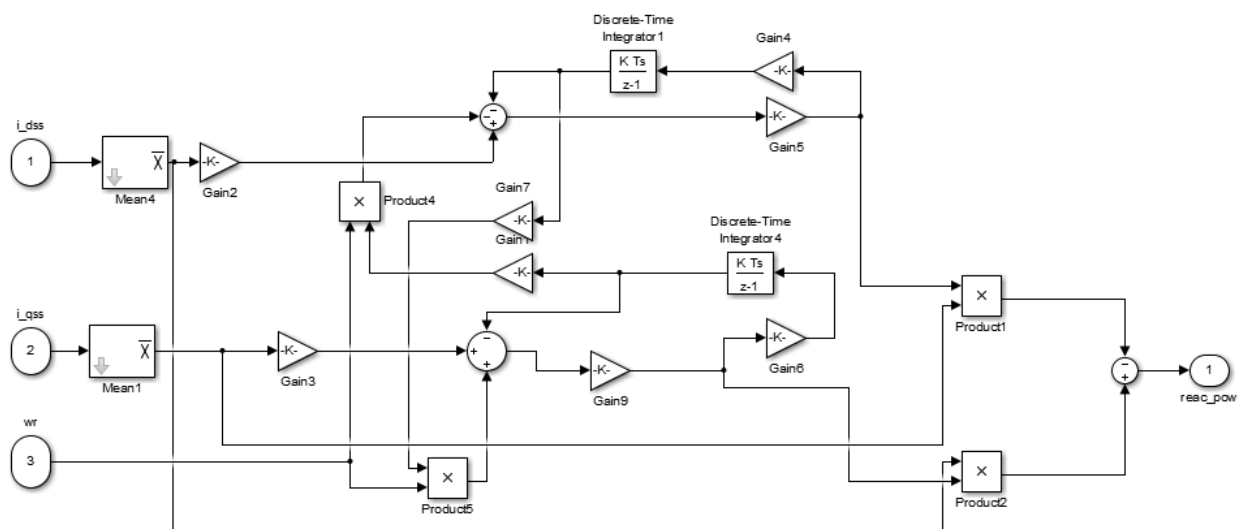


FIGURE 4.14: Simulink Adaptive model of Airgap power based MRAS

## Chapter 5

# RESULTS & DISCUSSIONS

---

The speed estimation is realized in the MATLAB/Simulink environment, using the Simpower system (SPS) toolbox under different operating conditions of VCIMD such as starting, load perturbation and speed reversal. The set of obtained response consists of reference speed ( $\omega_r^*$ ), estimated rotor speed ( $\omega_{est}$ ), actual rotor speed ( $\omega_r$ ), developed torque ( $T_r$ ), decoupled components of stator current space vector  $i_{ds}$ , and  $i_{qs}$ . The VCIMD uses PI controller as a speed controller. The current controller is realized using sinusoidal pwm technique.

### 5.1 STARTING DYNAMICS

The squirrel cage induction motor is fed from a current controlled VSI. The motor starts at low frequency decided by the controller and finally runs at steady state speed equal to the reference speed. The torque limit is set at twice the rated value to limit the output of the PI controller. The starting current is also inherently limited to the twice of the rated current value when the motor develops the required starting torque to reach the reference speed. On reaching steady state, the speed error reduces to zero, and the motor current falls to the no load value. The starting response obtained for induction motors rated 2HP and 30HP are shown in figure 5.1 to 5.14 for various speed estimation techniques. From the sensed motor currents ( $i_{as}, i_{bs}$ ) and DC link voltage ( $V_{DC}$ ) the rotor speed is estimated. The estimated speed and rotor speed are observed to be in close agreement, which proves the validity of the adopted estimation scheme.

5.1.1 Results Starting Dynamics

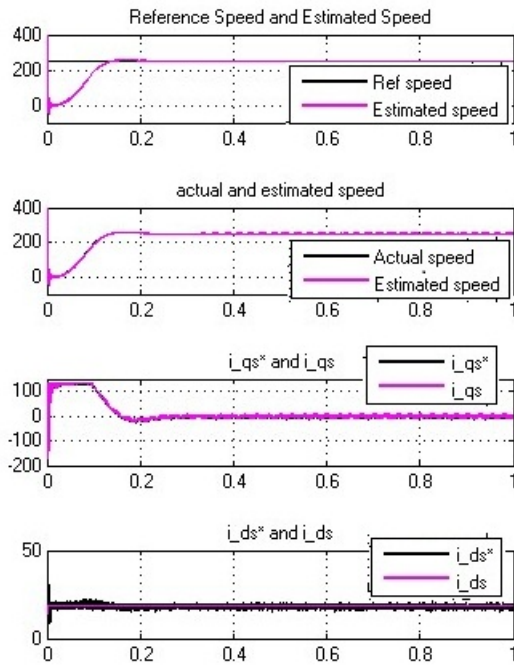


FIGURE 5.1: Starting dynamics of open loop speed estimator with  $\omega_r = 250\text{rad/sec}(30\text{hp})$

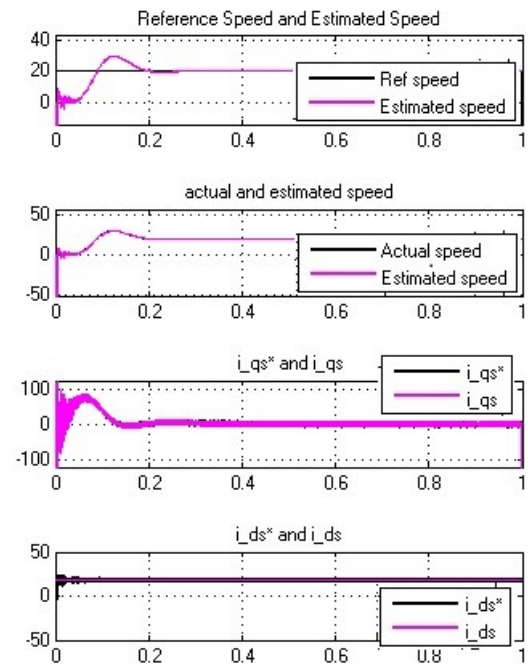


FIGURE 5.2: Starting dynamics of open loop speed estimator with  $\omega_r = 20\text{rad/sec}(30\text{hp})$

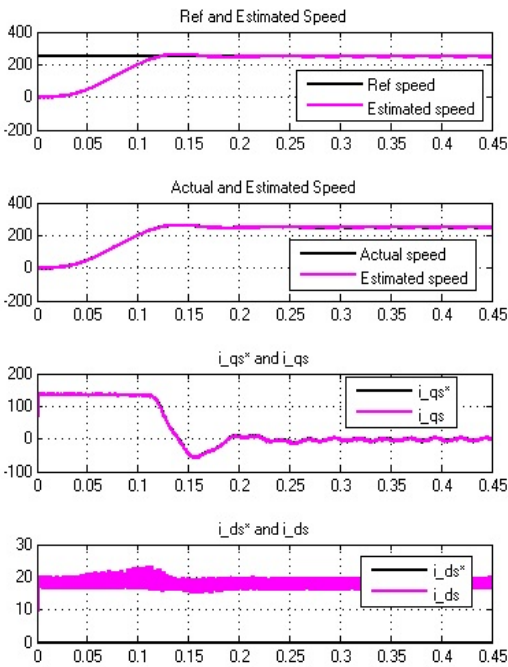


FIGURE 5.3: Starting dynamics of RF-based speed estimator with  $\omega_r = 250\text{rad/sec}(30\text{hp})$

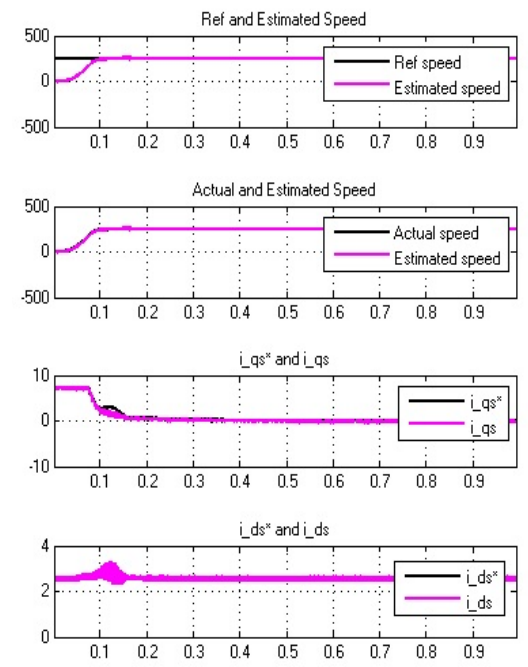


FIGURE 5.4: Starting dynamics of RF-based speed estimator with  $\omega_r = 20\text{rad/sec}(2\text{hp})$



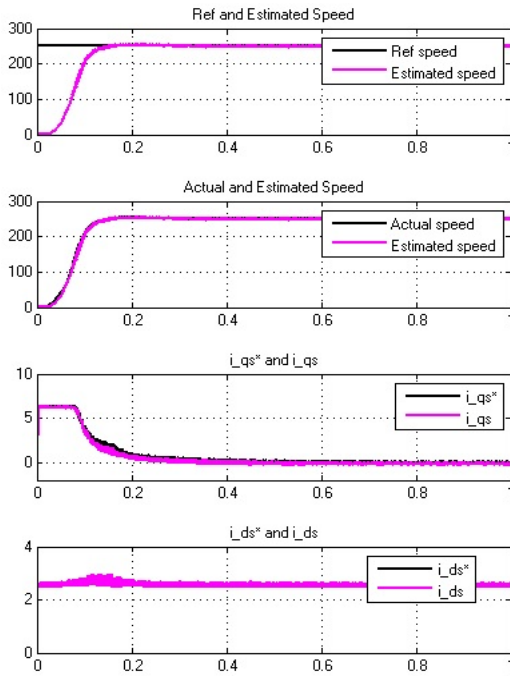


FIGURE 5.5: Starting dynamics of Back Emf based speed estimator with  $\omega_r = 250\text{rad/sec}(2\text{hp})$

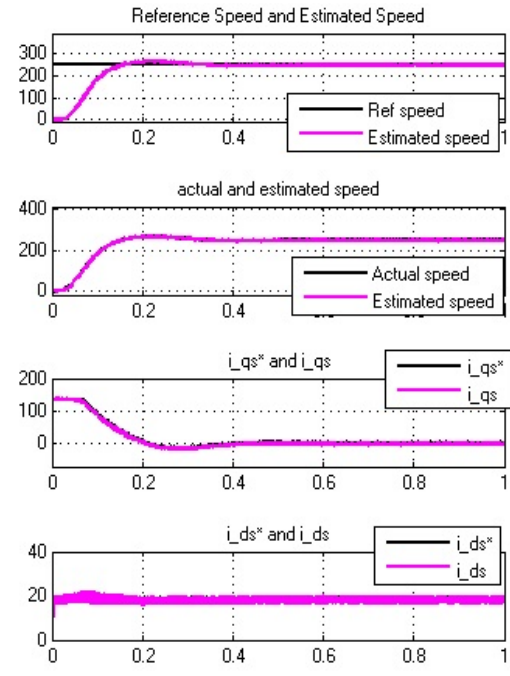


FIGURE 5.6: Starting dynamics of Back Emf based speed estimator with  $\omega_r = 250\text{rad/sec}(30\text{hp})$

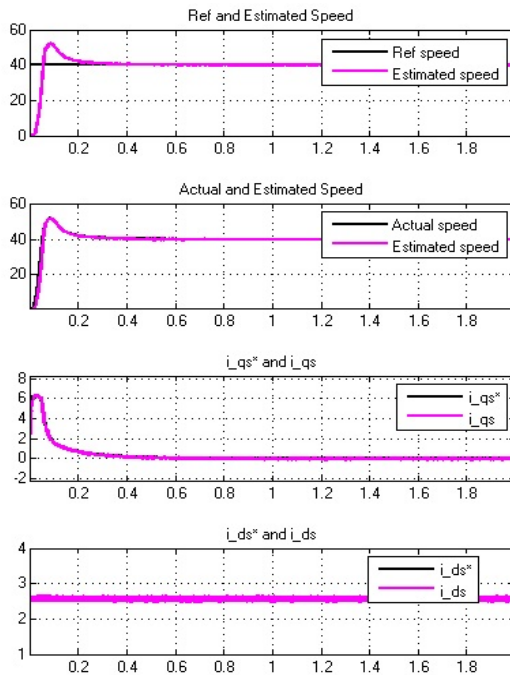


FIGURE 5.7: Starting dynamics of Back Emf based speed estimator with  $\omega_r = 40\text{rad/sec}(2\text{hp})$

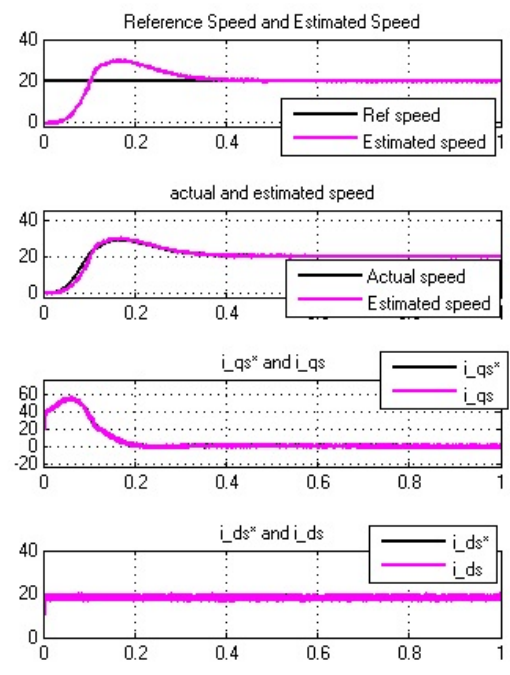


FIGURE 5.8: Starting dynamics of Back Emf based speed estimator with  $\omega_r = 20\text{rad/sec}(30\text{hp})$

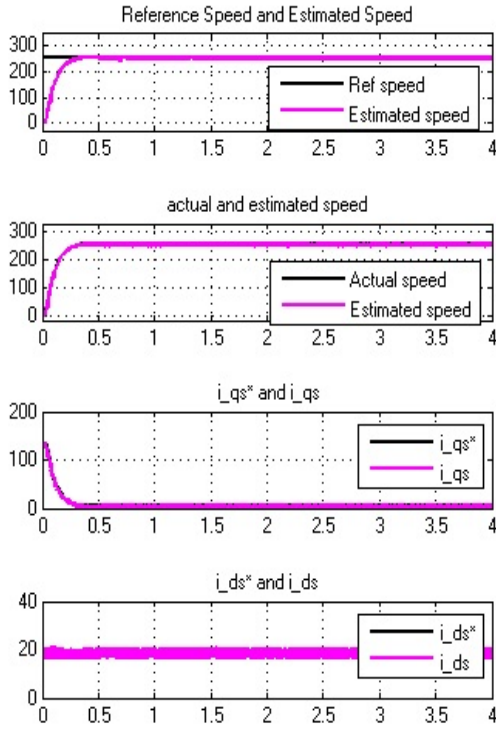


FIGURE 5.9: Starting dynamics of reactive power based speed estimator with  $\omega_r = 250\text{rad/sec}(30\text{hp})$

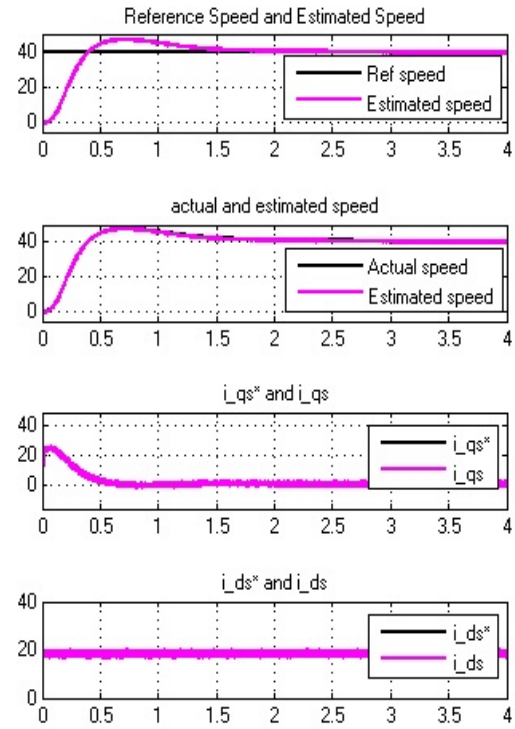


FIGURE 5.10: Starting dynamics of reactive power based speed estimator with  $\omega_r = 40\text{rad/sec}(30\text{hp})$

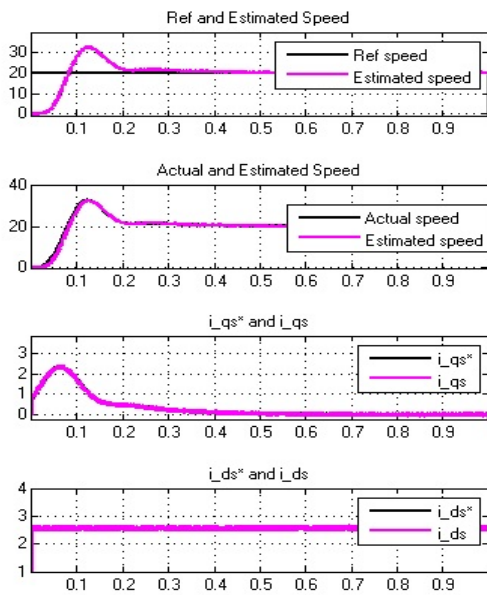


FIGURE 5.11: Starting dynamics of reactive power based speed estimator with  $\omega_r = 20\text{rad/sec}(2\text{hp})$

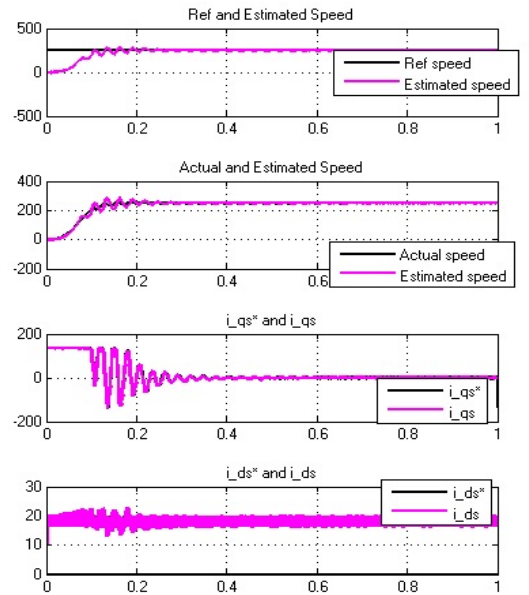


FIGURE 5.12: Starting dynamics of RF-based speed estimator with  $1.2R_s$  and  $\omega_r = 250\text{rad/sec}(30\text{hp})$

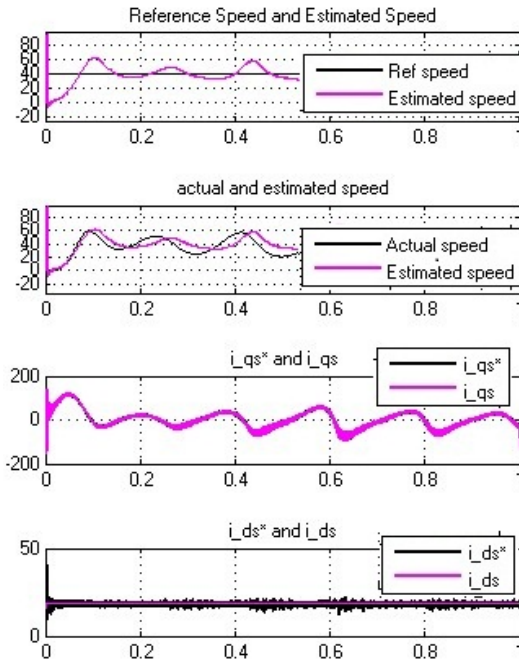


FIGURE 5.13: Starting dynamics of open loop speed estimator with  $1.2R_s$  and  $\omega_r = 40\text{rad/sec}(30\text{hp})$

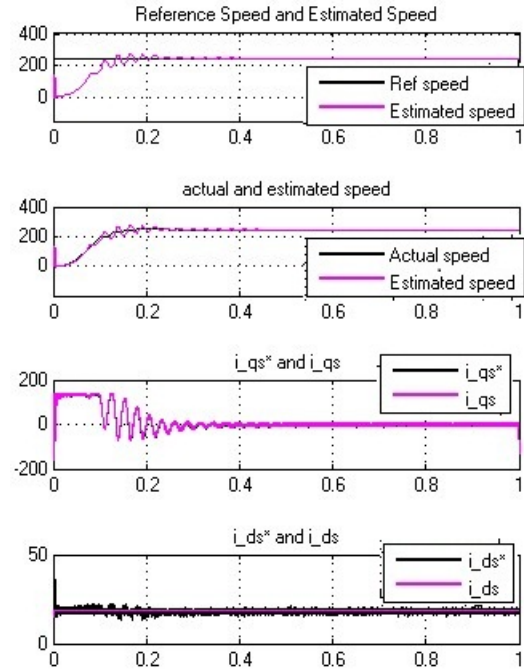


FIGURE 5.14: Starting dynamics of open loop speed estimator with  $1.2R_s$  and  $\omega_r = 250\text{rad/sec}(30\text{hp})$

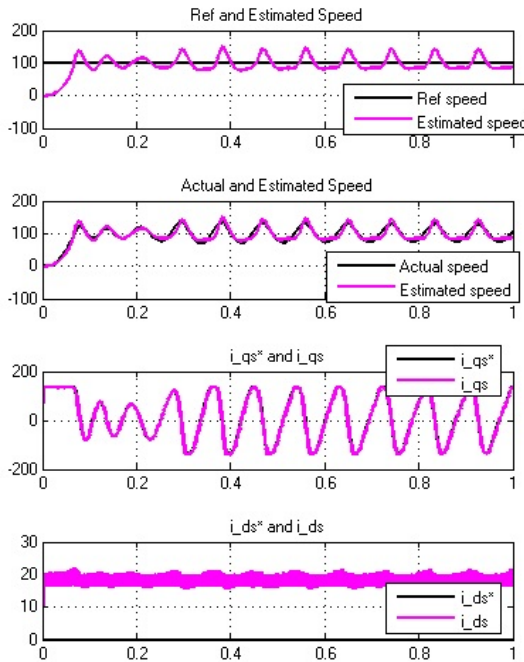


FIGURE 5.15: Starting dynamics of RF-based speed estimator with  $1.2R_s$  and  $\omega_r = 100\text{rad/sec}(30\text{hp})$

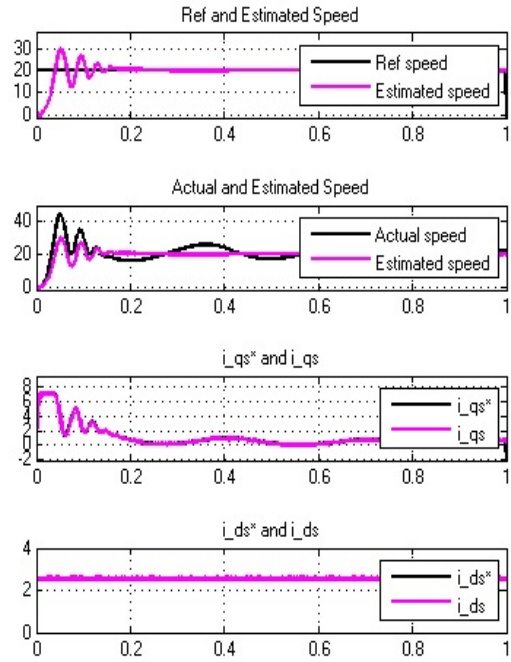


FIGURE 5.16: Starting dynamics of RF-based speed estimator with  $1.2R_s$  and  $\omega_r = 20\text{rad/sec}(2\text{hp})$

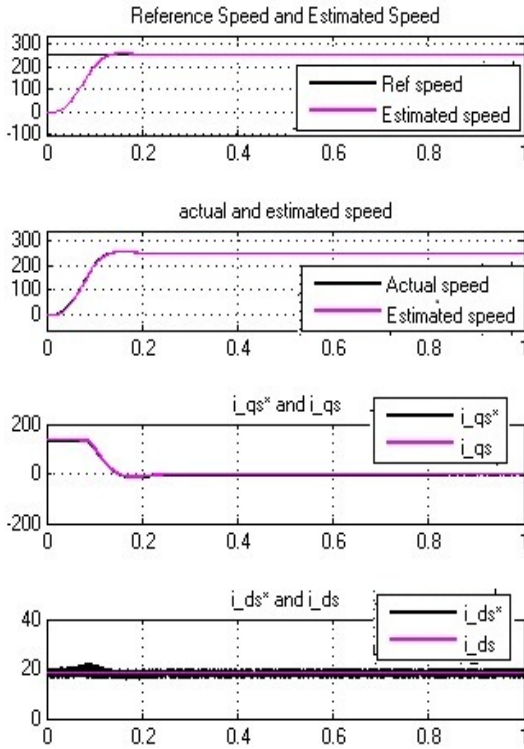


FIGURE 5.17: Starting dynamics of Back Emf based speed estimator with  $1.2R_s$  and  $\omega_r = 250\text{rad/sec}(30\text{hp})$

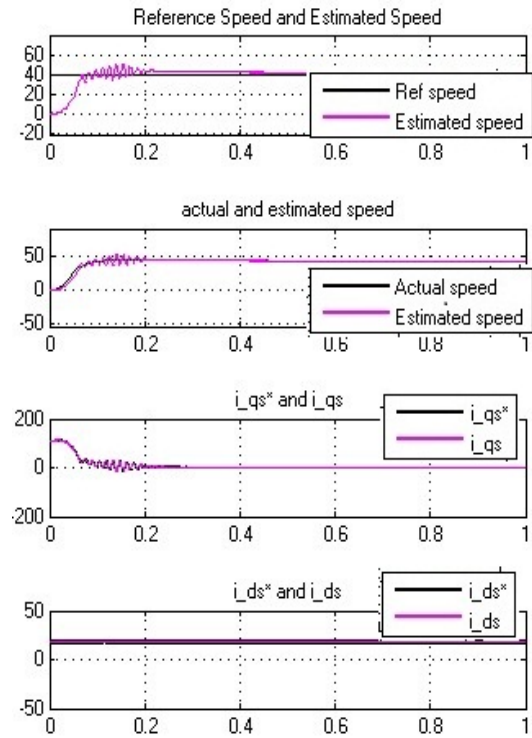


FIGURE 5.18: Starting dynamics of Back Emf speed estimator with  $1.2R_s$  and  $\omega_r = 40\text{rad/sec}(30\text{hp})$

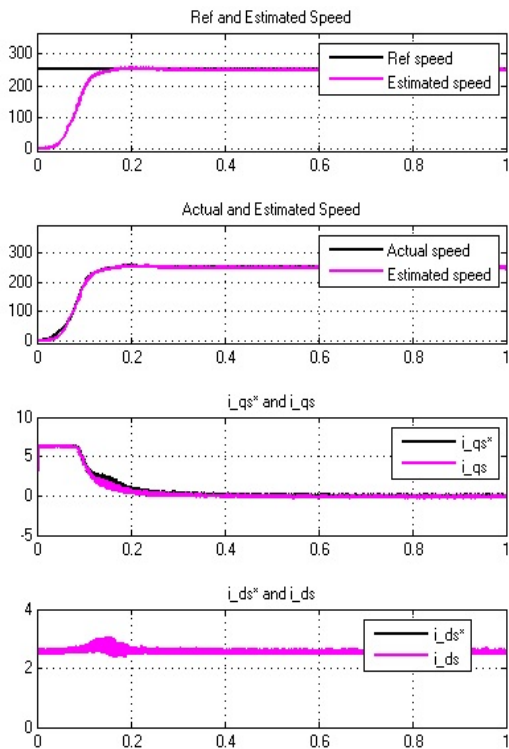


FIGURE 5.19: Starting dynamics of Bemf-based speed estimator with  $1.2R_s$  and  $\omega_r = 250\text{rad/sec}(2\text{hp})$

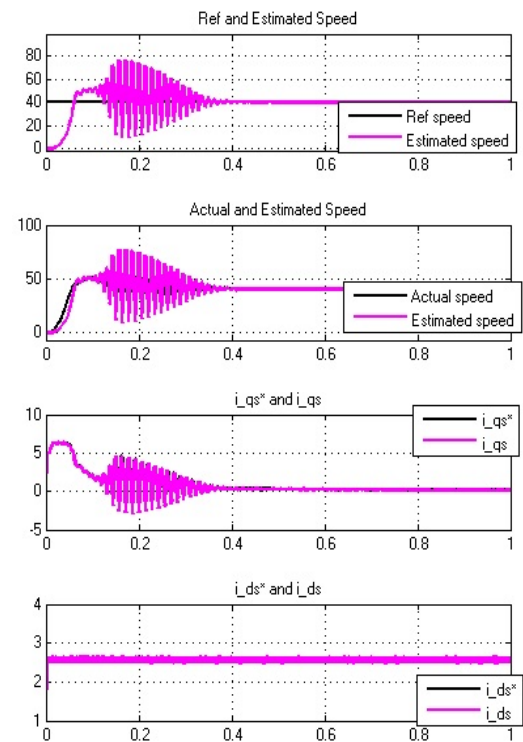


FIGURE 5.20: Starting dynamics of Bemf-based speed estimator with  $1.2R_s$  and  $\omega_r = 40\text{rad/sec}(2\text{hp})$

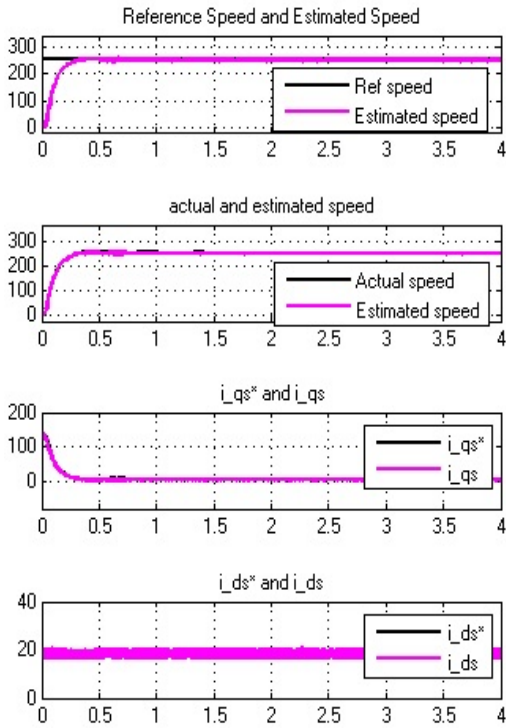


FIGURE 5.21: Starting dynamics of reactive power based speed estimator with  $1.2R_s$  and  $\omega_r = 250\text{rad/sec}(30\text{hp})$

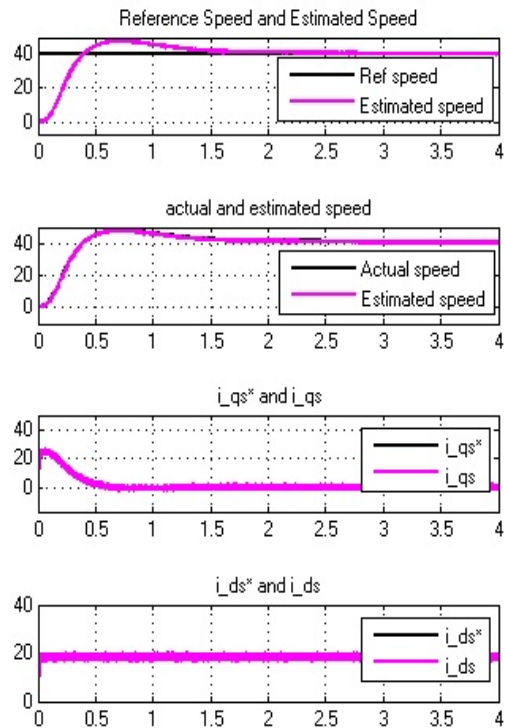


FIGURE 5.22: Starting dynamics of reactive power based speed estimator with  $1.5R_s$   $\omega_r = 40\text{rad/sec}(30\text{hp})$

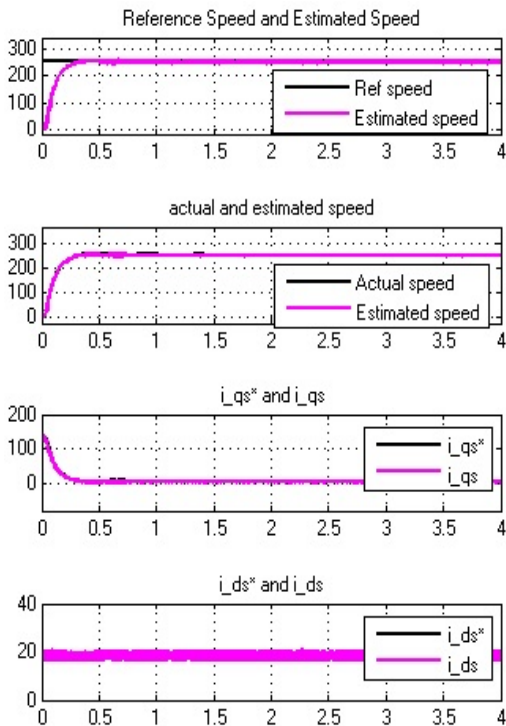


FIGURE 5.23: Starting dynamics of reactive power based speed estimator with  $1.5R_s$  and  $\omega_r = 250\text{rad/sec}(30\text{hp})$

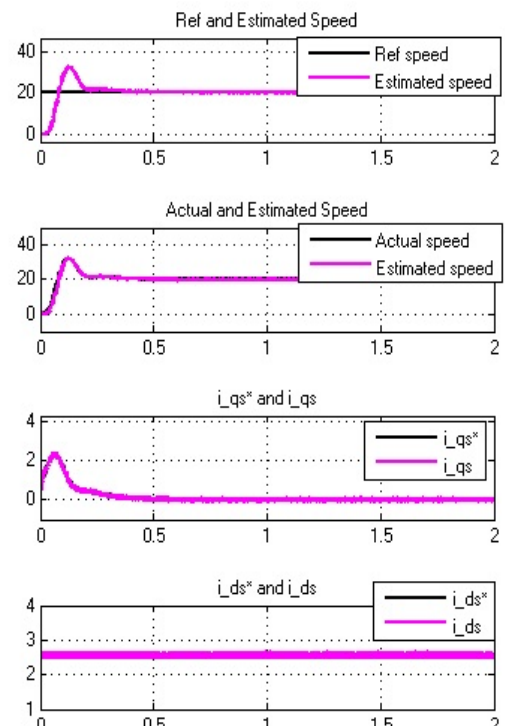


FIGURE 5.24: Starting dynamics of reactive power based speed estimator with  $1.5R_s$   $\omega_r = 20\text{rad/sec}(2\text{hp})$

## 5.2 LOAD PERTURBATION

The load perturbation response of the VCIMDs rated for 30hp and 2hp have been shown in 5.25 to 5.32. When the VCIMD is running at steady state, load torque is applied to the motor shaft. The sudden application in the load torque causes a small dip in motor speed, which is restored by close loop operation of the drive in VC mode. The estimated speed ( $\omega_{est}$ ) of the motor and rotor speed ( $\omega_r$ ) match each other showing the validity of the developed estimator algorithm.

While the VCIMD is operating at steady state under rated load, a sudden removal of the load torque from motor shaft results in the rotor speed above the set reference value. The estimated speed and rotor speed are observed to match each other in the dynamic response of the VCIMD.

### 5.2.1 Results of load Perturbation

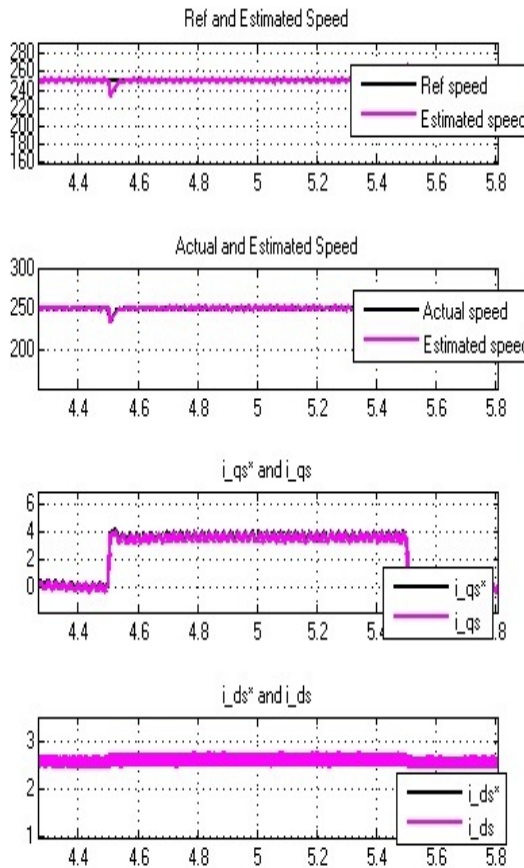


FIGURE 5.25: Load perturbation of RF-based speed estimator with  $\omega_r = 250\text{rad/sec}(2\text{hp})$

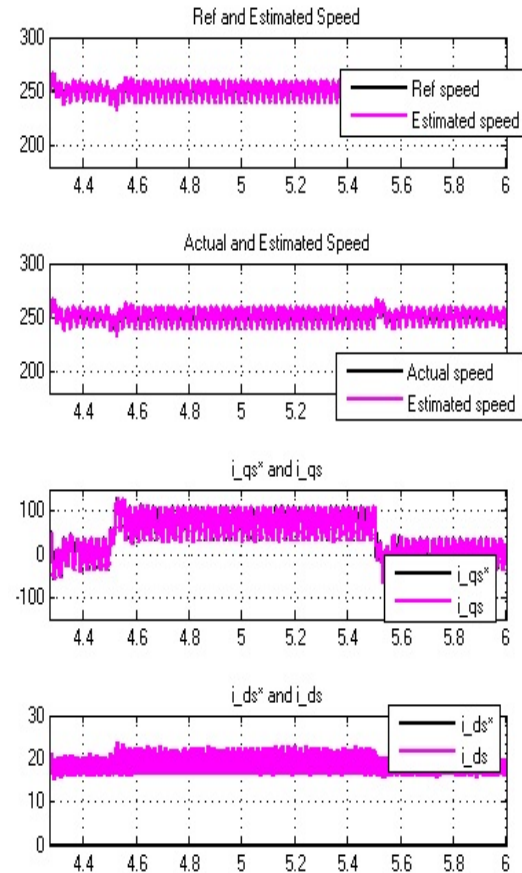


FIGURE 5.26: Load perturbation of RF-based speed estimator with  $\omega_r = 250\text{rad/sec}(30\text{hp})$

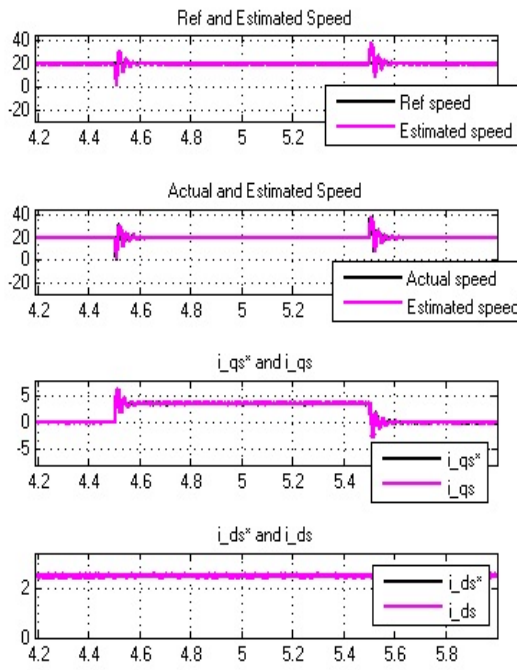


FIGURE 5.27: Load perturbation of RF-based speed estimator with  $\omega_r = 20\text{rad/sec}(2\text{hp})$

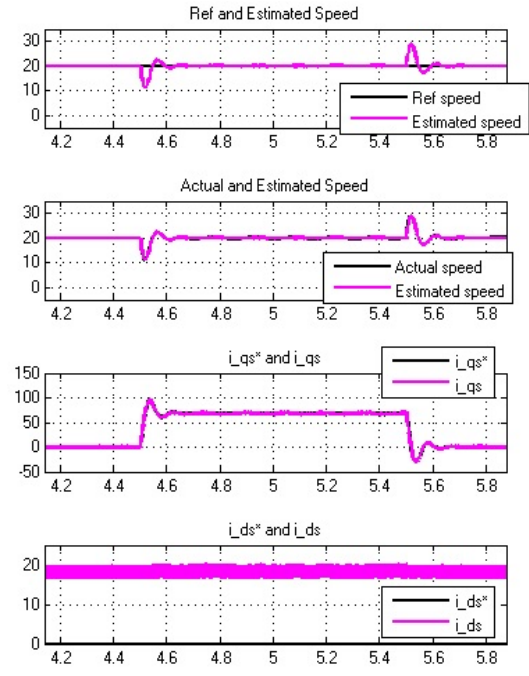


FIGURE 5.28: Load perturbation of RF-based speed estimator with  $\omega_r = 20\text{rad/sec}(30\text{hp})$

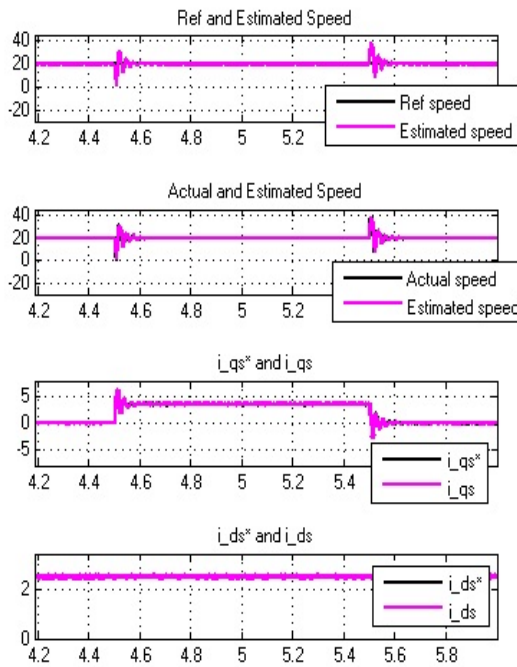


FIGURE 5.29: Load perturbation of Back Emf-based speed estimator with  $\omega_r = 20\text{rad/sec}(2\text{hp})$

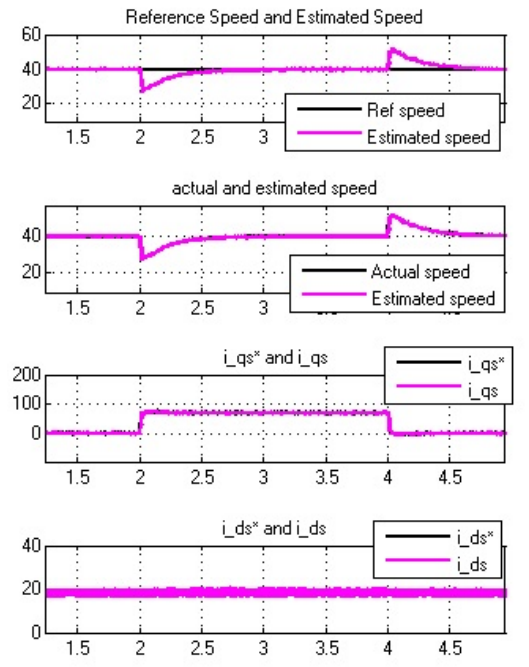


FIGURE 5.30: Load perturbation of Back Emf based speed estimator with  $\omega_r = 20\text{rad/sec}(30\text{hp})$

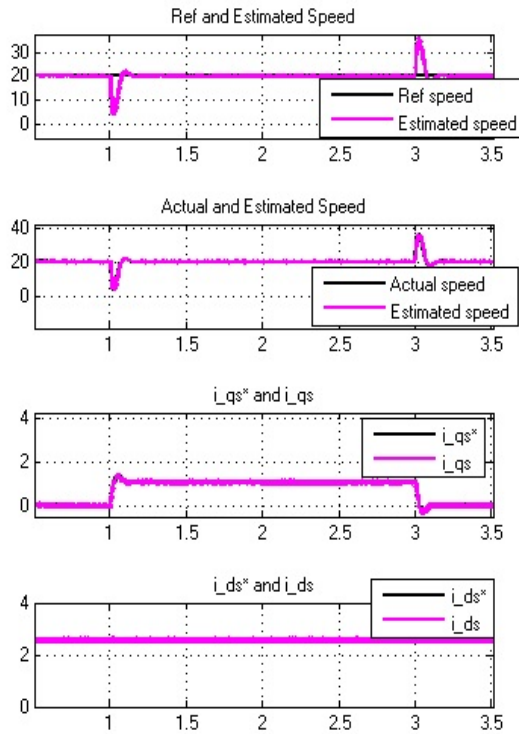


FIGURE 5.31: Load perturbation of reactive power based speed estimator with  $\omega_r = 20\text{rad/sec}(2hp)$

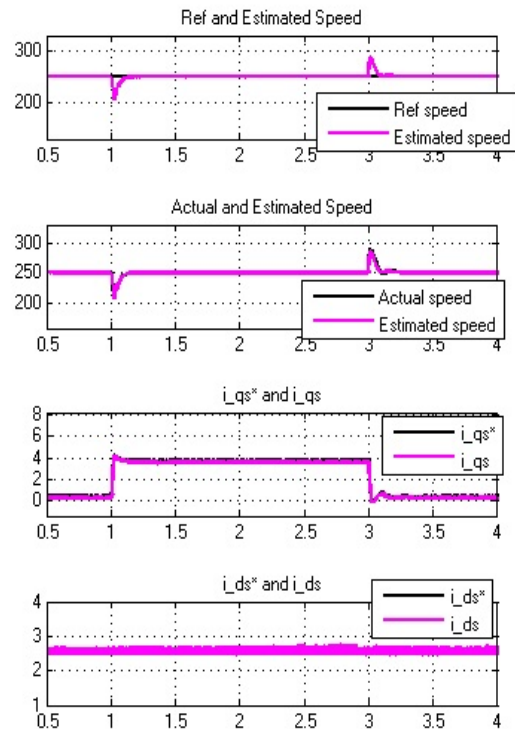


FIGURE 5.32: Load perturbation of Back Emf based speed estimator with  $\omega_r = 250\text{rad/sec}(2hp)$

### 5.3 FOUR QUADRANT OPERATION

The four quadrant operation operation for motors rated for  $30hp$  and  $2hp$  are shown in figure 5.33 to 5.38. When  $3 - \phi$  induction motor is running in VC mode at steady state, the reference value is changed to some negative value. In response to the applied change the controller reduces the frequency of the motor to start in reverse direction. Before and after the reversal phenomena, the drive is in the same dynamic state, therefore, the currents of the three phase induction motor in both the directions are observed to be same both in magnitude and frequency. The phase sequence observed in both the directions are opposite. The observed results show that the rotor speed and estimated rotor speed both overlap each other. The sequence of the response is in correlation to the estimated speed.



### 5.3.1 Results of Four Quadrant Operation of IM

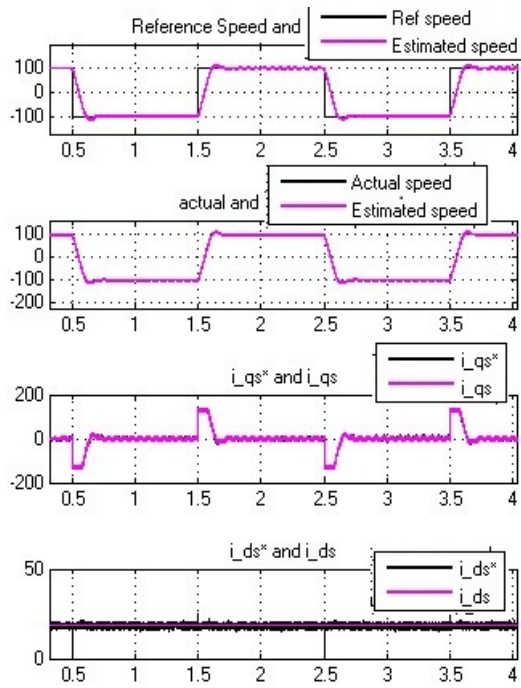


FIGURE 5.33: Performance of open loop speed estimator with  $\omega_r = \pm 100 \text{ rad/sec}(30 \text{ hp})$

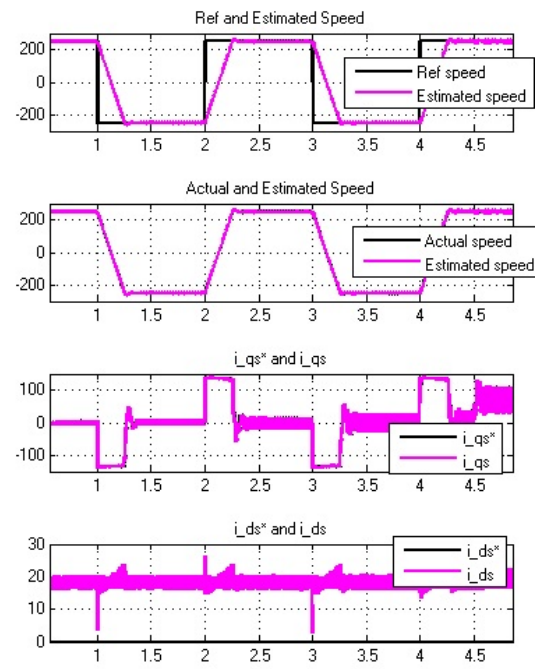


FIGURE 5.34: Performance of RF-based speed estimator with  $\omega_r = \pm 250 \text{ rad/sec}(30 \text{ hp})$

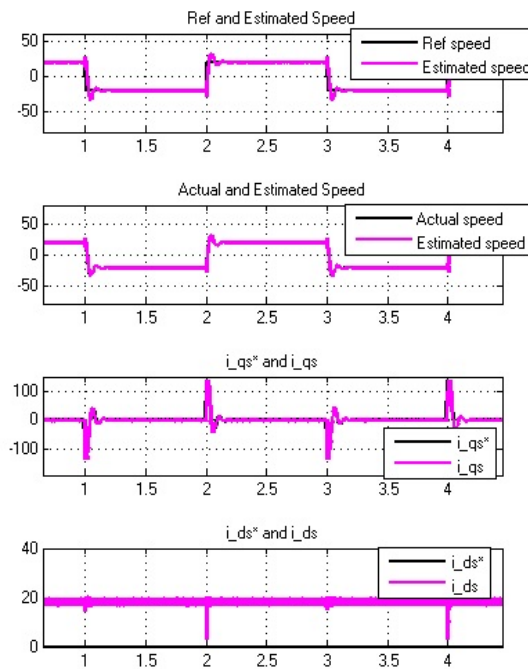


FIGURE 5.35: Performance of RF-based speed estimator with  $\omega_r = \pm 20 \text{ rad/sec}(30 \text{ hp})$

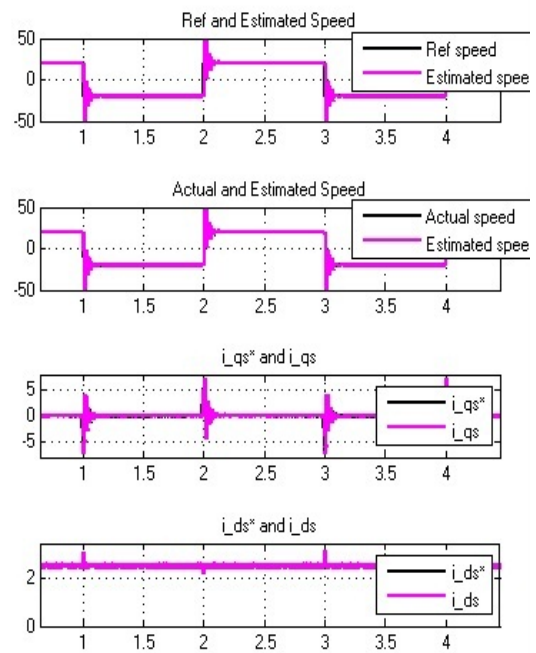


FIGURE 5.36: Performance of RF-based speed estimator with  $\omega_r = \pm 20 \text{ rad/sec}(2 \text{ hp})$

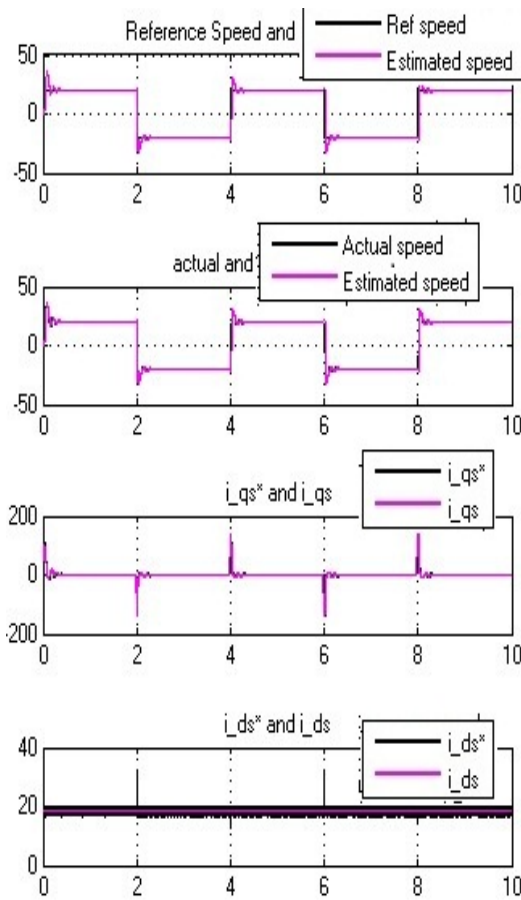


FIGURE 5.37: Performance of Back-Emf based estimator with  $\omega_r = \pm 20 \text{ rad/sec}(30 \text{ hp})$

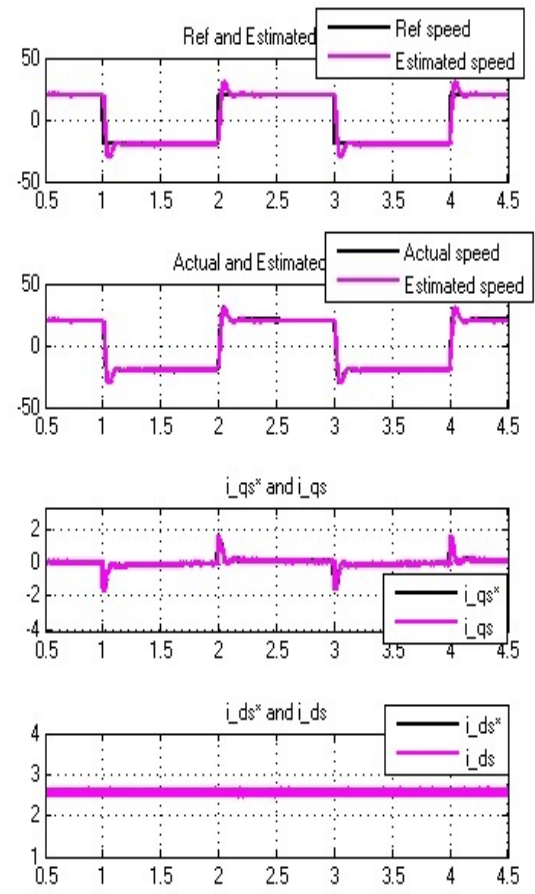


FIGURE 5.38: Performance of reactive power-based speed estimator with  $\omega_r = \pm 20 \text{ rad/sec}(2 \text{ hp})$

## Chapter 6

# CONCLUSIONS & FUTURE SCOPE OF WORK

---

### 6.1 CONCLUSIONS

Induction motor operated in vector controlled mode(VCM) is successfully implemented in MATLAB/SIMULINK environment using a PI controller with various speed estimation techniques. All the speed estimation techniques used here, demand only sensing of two phase currents and DC link voltage to estimate speed to complete the speed loop in a vector control induction motor drive.

Speed estimators like, open loop speed estimator, Rotor-flux based MRAS, back EMF based MRAS give accurate result at high speed as well as low speed as long as machine parameters specially stator resistance( $R_s$ ) are accurately known. As parameter changes during operation, performance of the aforesaid speed estimators deteriorates. The problem associated with stator resistance, has been eliminated using airgap-reactive power based MRAS. Now as other parameters like  $L_m$ ,  $L_r$  does not change much during operation of the induction motor, it is expected that reactive power based MRAS will work fine under various operating conditions which is validated through simulations. The use of speed estimator relieves drive from use of speed sensors, leading to the elimination of sensors and henceforth making system more robust.

## 6.2 FUTURE SCOPE OF WORK

Even though reactive power based MRAS speed estimation technique has shown its immunity against stator resistance variation of induction motor, its performance is effected with other parameter changes like  $L_m, L_r$  and specially  $R_r$ . So there is a scope in finding an algorithm where parameter dependancy becomes further less. Here PI controller is used as an adjustable mechanism which suffers from the disadvantage of overshoot, undershoot etc. It is expected that use of fuzzy or artificial intelligence (AI) based an adaptive mechanism can improve MRAS performance in an induction motor drive system.

# Bibliography

- [1] P. Krause, *Analysis of Electrical Machines and drives System*. Prentice Hall, 1985.
- [2] B. Bose, *Modern Power Electronics and AC drives*. Prentice Hall, 2002.
- [3] A.Hughes, "Vector control in cage motors-underlying mechanisms," *Vector Control Revisited (Digest No. 1998/199), IEE Colloquium on, London, 1998*, pp. 1/1–1/4, 1998.
- [4] J.A.Santisteban and R. Stephan, "Vector control methods for induction machines: an overview," *IEEE Transactions on Education*, vol. 44, no. 2, pp. 170–175, 2001.
- [5] H.Muhammad and Rashid, *Power Electronics Circuits, Devices and Applications*. Pearson Education, third Edition, 2004.
- [6] P.Vas, *Sensorless Vector and Direct Torque Control*. Oxford University Press, 1990.
- [7] W.leonard, *Control of Electric Drives*. New Delhi, Narosa Publications, 1985.
- [8] B.Ozpineci and L. M. Tolbert, "Simulink implementation of induction machine model - a modular approach," *Electric Machines and Drives Conference, 2003. IEMDC'03. IEEE International, 2003*, vol. 2, pp. 728–734, 2003.
- [9] W.Leonard, "Field orientation for controlling ac machines-principle and application," *in proc. 1988 Power Electronics and variable speed drives Conf.*, pp. 277–282, 1988.
- [10] F.Blashke, "The pinciple of field orientation as applied to the new transvector closed loop controlsystem for rotating-field machines," *Siemens Review*, vol. 34, no. 3, pp. 217–220, 1972.

- [11] G. Yang and T.H. Chin, "Adaptive speed identification scheme for vector controlled speed sensor-less inverter-induction motor drive," *Industry Applications Society Annual Meeting, 1991., Conference Record of the 1991 IEEE, Dearborn, MI, USA, 1991*, vol. 1, no. 4, pp. 404–408, 1991.
- [12] L. Xu, R. Yi, Z. Chaoyi, S. Huanqing, and Y. Yong, "On speed sensorless vector control system for induction motor based on estimating speed by torque current differential," *2008 27th Chinese Control Conference, Kunming*, pp. 728–734, 2008.
- [13] R. Blasco-Gimenez, G. Asher, M. Sumner, and K. Bradley, "Dynamic performance limitations for mras based sensorless induction motor drives. 2. online parameter tuning and dynamic performance studies," in *Electric Power Applications, IEE Proceedings-*, vol. 143, no. 2. IET, 1996, pp. 123–134.
- [14] T.-H. Chin, "Approaches for vector control of induction motor without speed sensor," *Industrial Electronics, Control and Instrumentation, 1994. IECON '94., 20th International Conference on, Bologna, 1994*, no. 5, pp. 1616–1620, 1994.
- [15] C. Schauder, "Adaptive speed identification for vector control of induction motors without rotational transducers," *IEEE Transactions on industry applications*, vol. 28, no. 5, pp. 4269–4275, 1992.
- [16] B. Singh and S. G. Choudhury, "speed sensorless control of vector controlled induction motor drive," *The ICFAI University Journal of Electrical and Electronics Engineering*, no. 2, 2008.
- [17] M.-H. Shin, D.-S. Hyun, S.-B. Cho, and S.-Y. Choe, "An improved stator flux estimation for speed sensorless stator flux orientation control of induction motors," *IEEE Transactions on Power Electronics*, vol. 15, no. 2, pp. 111–117, 2000.
- [18] S. Ogasawara; H. Akagi; A. Nabae, "The generalized theory of indirect vector control for ac machines," *IEEE transactions on industry applications*, pp. 470–478, 1998.
- [19] J. Murphy and F.G. Turnbull, *Power Electronic Control of AC Motors*. Oxford Pergamon Press, 1988.
- [20] B. Singh, B.N. Singh, B.P. Singh, A. Chandra, and K. Al-Haddad, "Unity power factor converter-inverter fed vector controlled cage motor drive without mechanical speed sensor," *Industrial Electronics, Control, and Instrumentation, 1995., Proceedings of the 1995 IEEE IECON 21st International Conference on, Orlando, FL, 1995*, vol. 1, pp. 609–614, 1994.

- [21] L. M. Burrows, D. S. Zinger, and M. E. Roth, "Field oriented control of induction motors," *Energy Conversion Engineering Conference IECEC-90. Proceedings of the 25th Intersociety, 1990.*, vol. 1, pp. 391–396, 1990.
- [22] Y.S.Lai, C.N.Liu, K. Y.Chang, Y.C.Luo, C.I.Lee, and C. H.Liu, "Sensorless vector controllers for induction motor drives," *Power Electronics and Drive Systems, 1997. Proceedings., 1997 International Conference on, 1997*, vol. 2, pp. 663–669, 1997.
- [23] Z. Wu, D. Zhi, and J. Ying, "Research on speed estimation algorithm for induction motor drive," in *Power Electronics and Motion Control Conference, 2004. IPEMC 2004. The 4th International*, vol. 3. IEEE, 2004, pp. 1387–1392.
- [24] Y. A. Zorgani, Y. Koubaa, and M. Boussak, "Sensorless speed control with mras for induction motor drive," in *Electrical Machines (ICEM), 2012 XXth International Conference on*. IEEE, 2012, pp. 2259–2265.
- [25] J. W. Finch and D. Giaouris, "Controlled ac electrical drives," *Industrial Electronics, IEEE Transactions on*, vol. 55, no. 2, pp. 481–491, 2008.
- [26] J. Holtz, "Methods for speed sensorless control of ac drives," *Sensorless Control of AC Motor Drives*, pp. 21–29, 1996.
- [27] X.Xu and D.W.Novotny, "Implementation of direct stator flux orientation control on a versatile dsp based system," *IEEE Transactions on Industry Applications*, vol. 27, no. 4, pp. 694–700, 1991.
- [28] K. Huang, Y. Zhang, S. Huang, and L. Xiao, "A mras method for sensorless vector control of induction motor based on instantaneous reactive power," in *Electrical Machines and Systems (ICEMS), 2010 International Conference on*. IEEE, 2010, pp. 1396–1400.
- [29] C.Ilas, A.Bettini, L.Ferraris, G.Griva, and F. Profumo, "Comparison of different schemes without shaft sensors for field oriented control drives," *Industrial Electronics, Control and Instrumentation, 1994. IECON '94., 20th International Conference on, Bologna*, vol. 30, pp. 1579–1588, 1994.
- [30] C.-M. Ta, T. Uchida, and Y. Hori, "Mras-based speed sensorless control for induction motor drives using instantaneous reactive power," in *Industrial Electronics Society, 2001. IECON'01. The 27th Annual Conference of the IEEE*, vol. 2. IEEE, 2001, pp. 1417–1422.

- [31] R. Kumar, S. Das, P. Syam, and A. K. Chattopadhyay, "Review on model reference adaptive system for sensorless vector control of induction motor drives," *Electric Power Applications, IET*, vol. 9, no. 7, pp. 496–511, 2015.
- [32] F.-Z. Peng and T. Fukao, "Robust speed identification for speed-sensorless vector control of induction motors," *IEEE Transactions on Industry Applications*, vol. 30, no. 5, pp. 1234–1240, 1994.
- [33] M. N. Marwali and A. Keyhani, "A comparative study of rotor flux based mras and back emf based mras speed estimators for speed sensorless vector control of induction machines," in *Industry Applications Conference, 1997. Thirty-Second IAS Annual Meeting, IAS'97., Conference Record of the 1997 IEEE*, vol. 1. IEEE, 1997, pp. 160–166.
- [34] A. R. Haron and N. R. N. Idris, "Simulation of mras-based speed sensorless estimation of induction motor drives using matlab/simulink," in *Power and Energy Conference, 2006. PECon'06. IEEE International*. IEEE, 2006, pp. 411–415.
- [35] M. Rashed, F. Stronach, and P. Vas, "A stable mras-based sensorless vector control induction motor drive at low speeds," in *Electric Machines and Drives Conference, 2003. IEMDC'03. IEEE International*, vol. 1. IEEE, 2003, pp. 139–144.
- [36] S. Maiti, C. Chakraborty, and S. SenGupta, "Adaptive estimation of speed and rotor time constant for the vector controlled induction motor drive using reactive power," in *Industrial Electronics Society, 2007. IECON 2007. 33rd Annual Conference of the IEEE*. IEEE, 2007, pp. 286–291.
- [37] S. Maiti, C. Chakraborty, Y. Hori, and M. C. Ta, "Model reference adaptive controller-based rotor resistance and speed estimation techniques for vector controlled induction motor drive utilizing reactive power," *Industrial Electronics, IEEE Transactions on*, vol. 55, no. 2, pp. 594–601, 2008.
- [38] C. Chakraborty, A. R. Teja, S. Maiti, and Y. Hori, "A new  $v \times i$  based adaptive speed sensorless four quadrant vector controlled induction motor drive," in *Power Electronics Conference (IPEC), 2010 International*. IEEE, 2010, pp. 3041–3048.
- [39] C. Chakraborty, M. C. Ta, and Y. Hori, "Speed sensorless, efficiency optimized control of induction motor drives suitable for ev applications," in *Industrial Electronics Society, 2003. IECON'03. The 29th Annual Conference of the IEEE*, vol. 1. IEEE, 2003, pp. 913–918.



- [40] A. Ravi Teja, V. Verma, and C. Chakraborty, "A new formulation of reactive-power-based model reference adaptive system for sensorless induction motor drive," *Industrial Electronics, IEEE Transactions on*, vol. 62, no. 11, pp. 6797–6808, 2015.
- [41] V. Verma and C. Chakraborty, "New series of mras for speed estimation of vector controlled induction motor drive," in *Industrial Electronics Society, IECON 2014-40th Annual Conference of the IEEE*. IEEE, 2014, pp. 755–761.
- [42] I. Benlaloui, S. Drid, L. Chrifi-Alaoui, and M. Ouriagli, "Implementation of a new mras speed sensorless vector control of induction machine," *Energy Conversion, IEEE Transactions on*, vol. 30, no. 2, pp. 588–595, 2015.
- [43] T.-S. Kwon, M.-H. Shin, and D.-S. Hyun, "Speed sensorless stator flux-oriented control of induction motor in the field weakening region using luenberger observer," *IEEE Transactions on Power Electronics*, vol. 20, no. 4, pp. 864–869, July 2005.
- [44] Y. Zhang, Z. Zhao, T. Lu, L. Yuan, W. Xu, and J. Zhu, "A comparative study of luenberger observer, sliding mode observer and extended kalman filter for sensorless vector control of induction motor drives," in *2009 IEEE Energy Conversion Congress and Exposition*, Sept 2009, pp. 2466–2473.
- [45] M. Barut, S. Bogosyan, and M. Gokasan, "Speed-sensorless estimation for induction motors using extended kalman filters," *IEEE Transactions on Industrial Electronics*, vol. 54, no. 1, pp. 272–280, Feb 2007.
- [46] Z. Wei and J. J. Luo, "Speed and rotor flux estimation of induction motors based on extended kalman filter," in *Networked Computing and Advanced Information Management (NCM), 2010 Sixth International Conference on*, Aug 2010, pp. 157–160.
- [47] B.N.Singh, *Ph.D dissertation, Dept. of Elec. Eng., Indian Institute of Technology, Delhi, India*, no. 2.
- [48] K. Rajashekara, A. Kawamura, and K. Matsuse, *Sensorless control of AC motor drives: speed and position sensorless operation*. IEEE press New York, 1996.
- [49] H. Tajima and Y. Hori, "Speed sensorless field-orientation control of the induction machine," *Industry Applications, IEEE Transactions on*, vol. 29, no. 1, pp. 175–180, 1993.

- 
- [50] A. Tripathi, A. M.Khambadkone, and S.K.Panda, "Speed sensorless control of ac machines using direct flux control scheme," *Power Electronics and Drive Systems, 2003. PEDS 2003. The Fifth International Conference on, 2003*, vol. 2, pp. 1647–1652, 2003.
- [51] M. Dybkowski and T. Orłowska-Kowalska, "Speed sensorless induction motor drive with magnetizing reactance estimation," in *Power Electronics and Motion Control Conference (EPE/PEMC), 2010 14th International*. IEEE, 2010, pp. T5–120.
- [52] F. Rashidi, "Sensorless speed control of induction motor derives using a robust and adaptive neuro-fuzzy based intelligent controller," in *Industrial Technology, 2004. IEEE ICIT'04. 2004 IEEE International Conference on*, vol. 2. IEEE, 2004, pp. 617–627.

# Appendix I

Specification of the induction motors considered in this report.

## **Cage Induction motor I**

30 HP, 3-phase, 2-pole, Y-Connected 415V, 50 HZ  $R_s = 0.251 \Omega$ ,  $R_r = 0.249 \Omega$ ,  
 $L_m = 0.0416$  henry,  $L_{ls} = 0.001397$  henry,  $L_{lr} = 0.001397$  henry,  $J = 0.305 \text{ Kgm}^2$

## **Cage Induction motor II**

2 HP, 3-phase, 4-pole, Y-Connected 415V, 50 HZ  $R_s = 5.4 \Omega$ ,  $R_r = 3.109 \Omega$ ,  $L_m =$   
 $0.38915$  henry,  $L_{ls} = 0.0284$  henry,  $L_{lr} = 0.0284$  henry,  $J = 0.00436 \text{ Kgm}^2$

# Appendix II

## PI controller values for 2hp motor

### RF-MRAS

$$\begin{aligned}k_p &= 0.3 & k_i &= 0.009 \\k_{pmras} &= 1000 & k_{imras} &= 600\end{aligned}$$

### Back-Emf MRAS

$$\begin{aligned}k_p &= 0.3 & k_i &= 0.001 \\k_{pmras} &= 0.3 & k_{imras} &= 1\end{aligned}$$

### Reactive Power MRAS

$$\begin{aligned}k_p &= 0.1 & k_i &= 0.005 \\k_{pmras} &= 0.01 & k_{imras} &= 0.0008\end{aligned}$$

## PI controller values for 30hp motor

### RF-MRAS

$$\begin{aligned}k_p &= 8 & k_i &= 0.08 \\k_{pmras} &= 1000 & k_{imras} &= 500\end{aligned}$$

### Back-Emf MRAS

$$\begin{aligned}k_p &= 12 & k_i &= 0.005 \\k_{pmras} &= 0.3 & k_{imras} &= 6\end{aligned}$$

### Reactive Power MRAS

$$\begin{aligned}k_p &= 0.2 & k_i &= 0.0005 \\k_{pmras} &= 0.01 & k_{imras} &= 0.008\end{aligned}$$